Hindawi
Journal of Advanced Transportation
Volume 2022, Article ID 6034369, 22 pages
https://doi.org/10.1155/2022/6034369

Research Article

Modeling Network Capacity for Urban Multimodal Transportation Applications

Xiaowei Jiang,[1] **Xiaonian Shan**,[2] **and Muqing Du**[2]

[1]*Jiangsu AI Transportation Innovations and Applications Engineering Research Center, Jinling Institute of Technology, Nanjing, China*
[2]*College of Civil and Transportation Engineering, Hohai University, Nanjing, China*

Correspondence should be addressed to Muqing Du; dumqhhu@hhu.edu.cn

Received 8 August 2022; Revised 11 September 2022; Accepted 19 September 2022; Published 6 October 2022

Academic Editor: Ziyuan Pu

Since the diversity of urban transport modes and the growth of public transport demands recently, it is essential to consider the multiple mode options in the network capacity problem. This paper derives a comprehensive network capacity model from a single-mode transportation network with only route choice to a multimodal transportation network with both mode choice and route choice. To avoid biases in the evaluation of the multimodal network capacity, two characteristics of the multimodal transportation system are considered in modeling and formulating the problem: (1) the mode interaction between cars and buses is explicitly reflected when they share the same link; (2) the correlation of travel alternatives (modes or routes) is measured by developing a combined modal split and traffic assignment (CMSTA) problem, in which the nested logit (NL) model is employed to account for mode similarity in mode split, while the path-size logit model (PSL) is employed to account for route overlapping in traffic assignment. Numerical experiments demonstrate the characteristics of the new model. It also shows how planning schemes or management strategies affect the multimodal transportation network capacity via a real network case.

1. Introduction

With the rapid urbanization in the newly-developing cities around the world, limited land and resources restrict the growth of supply capacity of the urban transportation system [1–3]. Most transportation networks were designed or managed for efficient and economical purposes, in which the transportation projects are supposed to use money, time, goods, etc. carefully and without wasting any. Economical design is preferred when the budget is of concerned [2, 4]. However, in consideration of the unexpected natural and man-made disasters, "plan some more" is needed to provide adequate spare capacity to make our transportation networks robust and resilient. To be more specific, sufficient capacity is vital for transportation networks when facing the planned and unplanned disruptions [5]. Spare transportation network capacity can prevent disruptions to cut off the critical lifelines in modern society, which can damage regional and national economic competitiveness and make peoples' lives difficult. On the other hand, an efficiency-priority design may cause the paradox of reducing network throughput Yang and Bell [6]. This finding suggested that consider the capacity-oriented analysis is another notable aspect of transportation network design and evaluation.

In the literature [5, 7–9], the transportation network capacity is defined to quantify the network-wide residual capacity with explicit consideration of travelers' destination, mode and/or route choice behaviors as well as congestion effect and level of service. In the literature, the transportation network capacity model was first derived in the road network. It can be regarded as an extended problem of the classical max-flow min-cut theorem by considering the travelers' realistic choice behavior in the passenger transportation network [10]. Wong and Yang [11] used a bilevel programming to characterize the reserve capacity of a traffic signal control network. Following that, Gao and Song [12] modified the Wong and Yang's reserve capacity model by using O-D specific multipliers. Similar modifications such as the ultimate

capacity model [13], and the practical capacity [9, 13], which assume the entire or partial O-D distribution is a variable with respect to the O-D travel costs. Besides, Wang et al. [14] proposed a logit-based stochastic user equilibrium with elastic demand (SUE-ED) for the estimation of the network throughput. However, the reserve capacity model is still a straightforward measure for network capacity estimation, and has been used in the literature [5, 15–17]. The reserve capacity is more suitable for the capacity estimation of a developed region where the O-D demand pattern will not vary too much.

With the development of the urban multimodal transportation system, it will be more meaningful to consider the multiple modes in the transportation capacity studies. Both Cheng et al. [18] and Xu et al. [5] consider the mode choice in the capacity assessment of the urban transportation systems. They only considered the competition between cars and rail transit, in which the passenger flow on the railway is independent of the traffic flow on the road network. Recently, Zheng et al. [19] explored the flexibility of the multimodal network capacity, which is measured by using a nested-logit (NL) based network capacity model. Liu et al. [20] modeled the multimodal network capacity problem by considering the second-best constraints. Ye et al. [21] proposed a bilevel programming model that can help to determine the location and capacity of the transfer infrastructure in the multimodal transportation system. Zhang et al. [22] proposed a network capacity model that considers the residual queues and the impact of the connected automated vehicles. Nevertheless, the above multimodal network capacity models did not consider the effects of mode similarities and flow interactions.

To properly model the multimodal transportation network capacity problem, it is necessary to consider the complexities involved in a multimodal transportation system, such as the mode attractiveness, which has a significant influence on mode share, the correlation among private and multiple public transport modes, and the vehicle interaction between private cars and public buses sharing the same roadway space. In short, the network capacity models developed to date are inadequate for estimating multimodal transportation network capacity assessment. Specifically, in the multimodal system, the physical separate modes can be simply considered as independent choice alternatives in mode split. However, some other travel modes, such as buses, may share the same physical links with the car mode, or even have interactions with car flows on the travel costs [23]. Adding the dependent modes could have an impact on the capacity of the original system. For the systems with more than two modes (either dependent or independent), except for the effect of sharing physical components, other external factors also cause correlations among different travel modes. For example, the public transport priority policy may correlate buses and subway; the travelers' attitude to traffic congestion may correlate bus and auto, which are both ground transportation. Empirically, the correlation of travel modes, referred to as *mode similarity*, affects the travel mode choice probabilities, and further influences the evaluation of the network capacity.

Furthermore, modelling travelers' behavior is another key to obtain an applicable and credible network capacity assessment for the multimodal urban transportation system. However, traditional multimodal equilibrium models did not consider this very well. The multimodal equilibrium problem belongs to the combined modal split and traffic assignment (CMSTA) model, which provides behavioral richness and computational tractability for characterizing the mode choice and route choice of travelers. The CMSTA model was first proposed by Florian and Nguyen [24] in which the transit mode was treated as exogenously given. Then, considering the mode split in the equilibrium process endogenously was presented as either variational inequality (VI) or fixed point (FP) formulations [25–27]. Further, the multinomial logit (MNL) model is used to characterize both mode choice and route choice behavior [28, 29]. However, the MNL model does have the issue of independence from irrelevant alternatives (IIA), which causes it cannot capture the effect of mode similarity and the route overlap in the urban multimodal transportation network [30, 31].

In this study, we model the multimodal transportation network capacity problem by considering multimodal choice options. The contributions of this study are as follows:

(i) To develop a new CMSTA model that characterizes the correlation of travel modes and routes in the assessment of multimodal transportation network capacity

(ii) To demonstrate the multimodal network capacity model for investigating how transportation planning or management strategies change the mode share rates and further affect the network-wide capacity

These improvements can help the administrators to better evaluate the network capacity of multimodal transportation systems. More specifically, an alternative CMSTA model will be conducted and adopted in the network capacity problem to capture multimodal behavior. The CMSTA model consists of a NL model in the phase of mode split and a path-size logit (PSL) model [32] in the phase of traffic assignment. Also, we provide an alternative MP formulation for the CMSTA model, in which the dual variables are referred to as the expected perceived costs (EPC) of the travel modes and the corresponding terms in objective function can be related to the entropy maximization theory. Thus, benefiting from the proposed multimodal network capacity model, this study be able to archive the two following goals of the network capacity assessment:

(i) How the effect of mode similarity and route overlap affects the network-wide capacity via the travelers' EPC of each subsystem in the multimodal transportation system

(ii) How transportation planning (e.g. adding a new link or new mode) and management strategies (e.g. raising the attractiveness of public transport) influence the multimodal transportation network capacity

On behalf of the above motivation, the remainder of this paper is organized as follows. The next section introduces

the multimodal network capacity problem, and then develop the formulation of the multimodal network capacity problem with the CMSTA model as its lower-level problem. In Section 3, a solution algorithm to the multimodal network capacity problem is provided based on the sensitivity analysis of the CMSTA model. Section 4 provides numerical examples to demonstrate the proposed model and remarkable findings.

2. Formulation of the Multimodal Network Capacity Problem

For the multimodal transportation system, the network capacity can be evaluated by finding the largest multiplier μ applied to a given O-D demand matrix that can be allocated to the multimodal transportation network without violating the capacity of any individual element from any travel mode. The product of the largest multiplier μ and the given O-D demand produces the maximum demand that can be allocated to the multimodal network. The value of multiplier μ hence indicates whether there is spare capacity to carry additional travel demand or not. In other words, the capacity of a multimodal network is bound by the lowest capacity of all travel modes.

Figure 1 illustrates the principle of the multimodal network capacity. As it shows, the travel demand grows like water flowing into the transportation system. The multimodal transportation network is represented as several connected containers. Each container represents a subnetwork of a travel mode. The multimodal system will be overflowed when the demand of any travel mode reaches its capacity. Furthermore, the *net travel impedance* [31] of each mode (evaluated by EPC of the mode *minus* its attractiveness) is another key factor to the total capacity. On one hand, the multimodal interactions and correlations influence the EPC of each travel mode; on the other hand, the travelers' preference determines the attractiveness of the modes. Thus, the choice of travel mode is the result of a trade-off between attractions and EPC. With the net travel impedance, the network-wide mode split can be decided, which further impacts the multimodal transportation network capacity. As Figure 1 shows, the net travel impedance determines the relative height of the container bottom, and further affects which mode will be filled in by the growing demand first. This implies modelling mode choice is the essence to the assessment of the multimodal network capacity problem. In the practical applications, the characteristics of the multimodal travel modes can be obtained by utilizing the advanced traffic information technology for calibrating the parameters in the multimodal network capacity model [2, 33].

Thereby, aiming to evaluate the capacity of transportation systems with multiple travel modes, a capacity model for multimodal transportation network will be formulated in this section. The model will be mathematically formulated as a bilevel program, in which the upper-level problem aims to maximize the total travel demand by all modes and the lower-level problem regulates the flow pattern in the multimodal transportation system. Specifically, the lower-level mathematical program (MP) is formulated as a combined mode split and traffic assignment (CMSTA) problem, in which the total travel demand is given under the capacity constraints from the upper-level model. In the CMSTA model, a nested logit (NL) model will be adopted to model the mode similarity, while the path-size logit (PSL) model is used to account for route overlapping.

2.1. Upper-Level Model. Based on the concept of *reserve capacity* for transportation network [5, 11], the upper level of the multimodal network capacity model will be formulated as a flow maximization problem:

$$\max_{\mu} \mu \tag{1}$$

$$\text{s.t.} v_a^m(\mu) \le \varphi_a^m C_a^m, \forall a \in A, m \in M, \tag{2}$$

$$q_{rs}^m(\mu) \le Q_{rs}^m, \forall m \in M, r \in R, s \in S, \tag{3}$$

where v_a^m is the traffic flow on link a by mode m; φ_a^m is the maximum flow-to-capacity ratio on link a by mode m; C_a^m is the capacity of link a serving mode m; Q_{rs}^m is the capacity of travel mode m between O-D pair (r, s), which can be related to the maximum rate of the transit service, such as buses or subway. Note that the constraints (2) and (3) exhibit nonlinear relationships, as the link flows and mode-specific O-D demands are implicit functions of the multiplier μ, of which the relationships are given in the lower-level problem of the bilevel model.

2.2. Lower-Level Model. This section develops the combined NL-PSL model for the CMSTA problem. Before formulating the NL-PSL model, we start with a generalization of the stochastic user equilibrium model with elastic demand (SUE-ED). Using the excess demand formulation to transform the elastic demand into a modal split [31]; the combined model with bimodal choice is further obtained. Figure 2 illustrates the idea of developing the bimodal demand model based on the elastic (excess) demand model. In this stage, we consider both independent modes and dependent modes which are corresponding to using separate networks (e.g., car and metro) or shared networks (e.g., car and bus), respectively. Hence, the issue of multimodal interaction can be figured out.

2.2.1. Elastic Demand Model for Car Network. This section presents a formulation of the single-modal elastic demand model with the logit-based SUE. The earliest elastic demand model was presented to incorporate with the standard user equilibrium (UE) [31]. Unlike the UE model assuming the O-D travel demand is fixed, the elastic demand model relaxes the fixed O-D demand assumption by considering it as a function of the minimum O-D travel costs. A demand function is consequently defined, in which the amount of O-D demand, q_{rs}, is decreasing with respect to the O-D travel cost, π_{rs}, i.e.,

$$q_{rs} = D_{rs}(\pi_{rs}), \forall r \in R, s \in S. \tag{4}$$

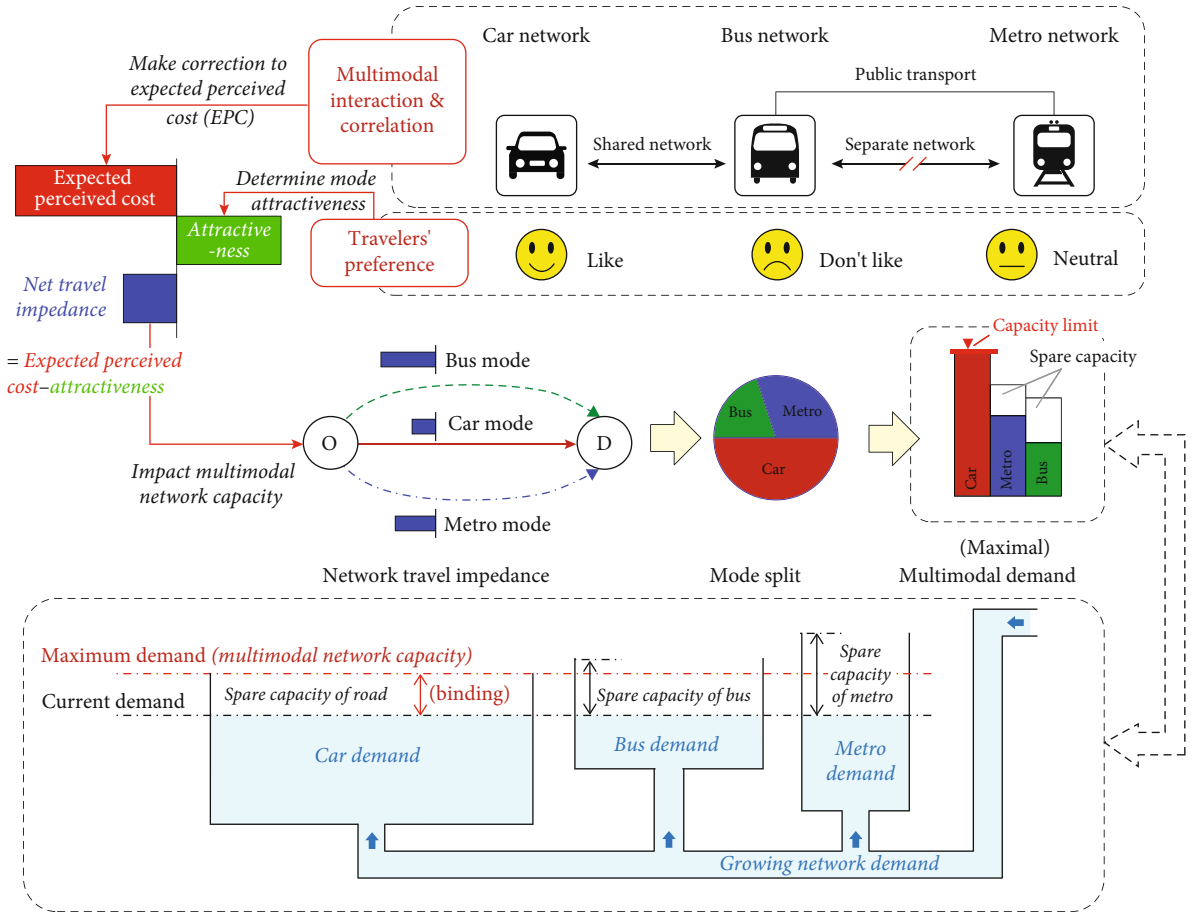

Figure 1: Concept of the network capacity analysis for multimodal transportation system.

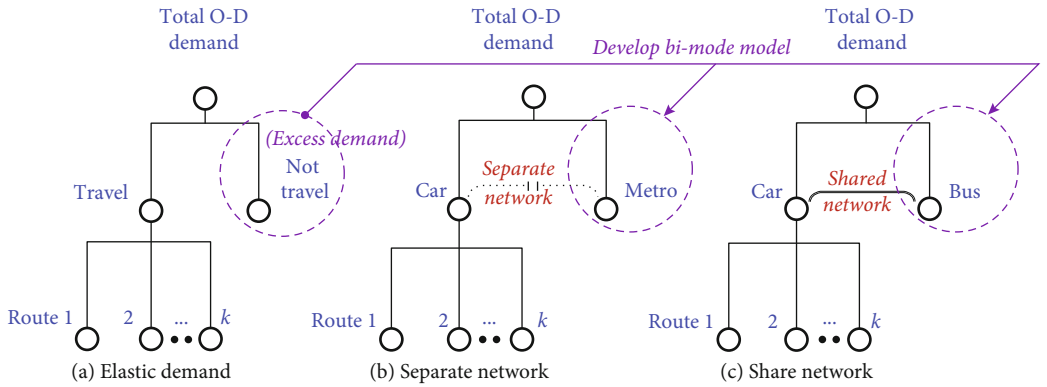

Figure 2: Similar structures for elastic demand model and bimodal models.

With its inverse function, i.e., $\pi_{rs} = D_{rs}^{-1}(q_{rs})$, the equilibrium of O-D demands is often described as the balance of supply and demand at the network level [31]. When the UE model is extended to the SUE model, the minimum O-D cost, π_{ij}, is replaced by the EPC of the O-D pair, w_{ij}, which is consistent with the SUE travelers' choice behavior based on the extreme value theory. The SUE-ED model can be formulated as the following MP by assuming the logit-based random utilities [34].

$$\min_{(f_k^{rs},q_{rs})} \sum_a \int_0^{v_a} t_a(x)dx - \sum_{rs} \int_0^{q_{rs}} D_{rs}^{-1}(v)dv + \frac{1}{\theta_k}\left(\sum_{rs}\sum_k f_k^{rs} \ln f_k^{rs} - \sum_{rs} q_{rs} \ln q_{rs}\right), \quad (5)$$

$$s.t. \sum_k f_k^{rs} = q_{rs}, \forall k \in K_{rs}, r \in R, s \in S, \quad (6)$$

$$v_a = \sum_{rs}\sum_k f_k^{rs} \delta_{ak}^{rs}, \forall a \in A, \quad (7)$$

$$f_k^{rs} \geq 0, \forall k \in K_{rs}, r \in R, s \in S, \tag{8}$$

$$0 < q_{rs} \leq \mu \bullet \bar{q}_{rs}, \forall r \in R, s \in S, \tag{9}$$

where f_k^{rs} is the flow on route k between O-D pair (r, s); θ_K is the scale parameter of the multinomial logit (MNL) model associated with stochastic route choice; δ_{ak}^{rs} is the link/route incidence parameter, and equal to 1 if route k (from r to s) travels through link a; 0 otherwise. $\{\bar{q}_{rs}\}$ is given as a prescribed O-D matrix for the computation of network capacity, while the multiplier μ is determined in the upper-level problem. $\mu \bullet \bar{q}_{rs}$ is the maximum potential demand that can be raised from r to s, as the O-D demand must be finite when the EPC drops to zero. To fulfill this property, a typical definition of demand function employs the negative exponential function, which has been adopted in Xu and Chen [34], Yang [35] and Sun et al. [36]. Besides, $t_a(v_a)$ is the link travel time function for link a, and is assumed strictly increasing and once continuously differentiable in its traffic flow v_a.

Remark 1. Note that the objective function of the SUE-ED model in Eq. (5) is organized as three separate terms. The first two terms are associated with the measure of total network congestion and elastic demand, respectively. These two terms are the same as the classical elastic (or variable) demand model for deterministic user equilibrium [31]. The last term is associated with the entropy maximization for stochastic equilibrium. The entropy maximization term is derived as follows.

Following the entropy maximization for trip distribution in Sheffi [31], the entropy of O-D demand is associated with the number of possible combinations resulting from each route choice decisions:

$$\prod_{rs} \frac{q_{rs}!}{\prod_k f_k^{rs}!} = \frac{\prod_{rs} q_{rs}!}{\prod_{rs} \prod_k f_k^{rs}!}. \tag{10}$$

By using the logarithmic transformation and Stirling's approximation (i.e., $\ln(x!) \approx x(\ln x - 1)$), the entropy maximization is equivalent to

$$\begin{aligned} &\max \sum_{rs} \ln(q_{rs}!) - \sum_{rs} \sum_k \ln(f_k^{rs}!) \approx \max \sum_{rs} q_{rs} \ln(q_{rs} - 1) - \sum_{rs} \sum_k f_k^{rs} \ln(f_k^{rs} - 1) \\ &= \max \sum_{rs} q_{rs} \ln q_{rs} - \sum_{rs} \sum_k f_k^{rs} \ln f_k^{rs} + \underbrace{\left(-\sum\nolimits_{rs} q_{rs} + \sum\nolimits_{rs} \sum\nolimits_k f_k^{rs}\right)}_{0} \\ &= \max \sum_{rs} q_{rs} \ln q_{rs} - \sum_{rs} \sum_k f_k^{rs} \ln f_k^{rs} \overset{equivalent\ to}{\longrightarrow} \min \sum_{rs} \sum_k f_k^{rs} \ln f_k^{rs} - \sum_{rs} q_{rs} \ln q_{rs}. \end{aligned} \tag{11}$$

It is worthy to note that the O-D demand q_{rs} is a function of the O-D travel cost in elastic demand model. Thus, the entropy maximization term in Eq. (5) is obtained. In addition, θ_K is the dispersion parameter that is associated with the perceptions travel costs of the travelers.

Based on Maher [37], the elastic demand model assumed the O-D travel demand is endogenous, which generates a flexible O-D pattern compared with the standard UE model with fixed O-D demand. With the upper-limit of demand for each O-D pair, the gap between the maximum and the equilibrated demand can be regarded as the portion of travelers that do not choose to travel on the network. This portion of travel demand is also referred to as the excess demand, denoted by e_{rs}. The objective function of the elastic demand model represented with excess demand can be given by

$$\begin{aligned} \min_{(f_k^{rs}, e_{rs})} &\sum_a \int_0^{v_a} t_a(w)\mathrm{d}w + \sum_{rs} \int_0^{e_{rs}} W_{rs}(v)dv + \frac{1}{\theta_K} \sum_{rs} \sum_k f_k^{rs} \ln f_k^{rs} \\ &- \frac{1}{\theta_K} \sum_{rs} \left(\sum_k f_k^{rs}\right) \ln \left(\sum_l f_l^{rs}\right), \end{aligned} \tag{12}$$

where $W_{rs}(e_{rs})$ equals to $D_{rs}^{-1}(q_{rs})$ by definition, and $\sum_k f_k^{rs} + e_{rs} = \mu \bullet \bar{q}_{rs}$. Besides, the above objective function subjects to the constraints (7) and (8) and the nonnegative constraint, $e_{rs} \geq 0$ $(\forall r, s)$.

It is worth to mention that, for a single modal network, alternative routes can be introduced by adding new links. However, in some cases, the total network capacity may not increase as expected, which is known as "*network capacity paradox*", see Yang and Bell [6] for details. Hence, our study suggests that adding alternative modes could be a better option if the decision-makers need to promote the transportation system capacity. The formulation for the multimodal network assignment will be derived in the remaining subsections.

2.2.2. Combined Model for Bimodal Network. In this subsection, the bimodal demand model will be developed based on the formulation of the excess demand model. The cases of independent modes and dependent modes are considered by using separate network representation and shared network representation, respectively.

(1) Separate Network. Based on the elastic demand model with respect to the excess demand, Sheffi [31] extended the UE model with elastic demand by replacing the demand function with a binary logit function. In the bimodal model, the excess demand is interpreted as the alternative travel mode (for example, public transit) which is independent to the original road network. The excess demand of the primary travel mode (for example, car) will transfer to the alternative mode. To properly balance the demand between the two modes, extra parameters are introduced, such as the EPC and the attractiveness of the alternative mode. A typical formulation is given as follows:

$$W_{rs}\left(q_{rs}^t\right) = \frac{1}{\theta_M} \ln \left(\frac{q_{rs}^t}{q_{rs}^{total} - q_{rs}^t} + w_{rs}^t - \Psi_{rs}^t\right), \tag{13}$$

where w_{rs}^t is the expected O-D travel cost by public transit; Ψ_{rs}^t is the exogenous attractiveness of the transit mode; q_{rs}^t is referred to as the demand of traveling by transit mode (in place of the excess demand e_{rs}); θ_M is the scale parameter for mode choice. Note that Ψ_{rs}^t is a constant that indicates the attractiveness of transit mode: $\Psi_{rs}^t > 0$ means that the

transit mode is more attractive than the car mode for O-D pair (r, s) given the condition that the car and bus mode take the same travel time.

Based on Eq. (13), the bimodal model can be formulated by following the excess demand model by Eq. (12):

$$\min_{(f_k^{rs}, q_{rs}^t)} \sum_a \int_0^{v_a} t_a(w)dw + \sum_{rs} \int_0^{q_{rs}^t} \left(\frac{1}{\theta_M} \ln \frac{w}{q_{rs}^{total} - w} + w_{rs}^t - \Psi_{rs}^t \right) dv, \tag{14}$$

$$+ \frac{1}{\theta_K} \sum_{rs} \sum_k f_k^{rs} \ln f_k^{rs} - \frac{1}{\theta_K} \sum_{rs} \left(\sum_k f_k^{rs} \right) \ln \left(\sum_l f_l^{rs} \right), \tag{15}$$

$$s.t. \sum_k f_k^{rs} + q_{rs}^t = q_{rs}^{total}, \forall r \in R, s \in S, \tag{16}$$

$$v_a = \sum_{rs} \sum_k f_k^{rs} \delta_{ak}^{rs}, \forall a \in A, \tag{17}$$

$$\mu \bullet \bar{q}_{rs} = q_{rs}^{total}, \forall r \in R, s \in S, \tag{18}$$

$$0 < q_{rs}^t \le q_{rs}^{total}, \forall r \in R, s \in S, \tag{19}$$

$$f_k^{rs} \ge 0, \forall k \in K_{rs}, r \in R, s \in S. \tag{20}$$

In the bimodal model for separate network, the last two terms of the objective function by Eq. (15) represent the entropy optimization for stochastic route choices.

Proposition 1. *Let π_{rs} be the dual variable associated with constraint (16), the optimal solution of π_{rs} represents the EPC by car mode from origin r to destination s. It is given by*

$$w_{rs}^{car} = \pi_{rs} = -\frac{1}{\theta_K} \ln \sum_l \exp\{-\theta_K c_l^{rs}\} \tag{21}$$

Proof. The Lagrange of the MP problem in Eqs. (15)–(20) is given by

$$L(f_k^{rs}, q_{rs}^t, \pi_{rs}) = \sum_a \int_0^{\sum_{rs} \sum_k f_k^{rs} \delta_{ak}^{rs}} t_a(w)dw + \sum_{rs} \int_0^{q_{rs}^t} \left(\frac{1}{\theta_M} \ln \frac{w}{q_{rs}^{total} - w} + w_{rs}^t - \Psi_{rs}^t \right) dv + \frac{1}{\theta_K} \sum_{rs} \sum_k f_k^{rs} \ln f_k^{rs} - \frac{1}{\theta_K} \sum_{rs} \left(\sum_k f_k^{rs} \right) \ln \left(\sum_l f_l^{rs} \right) + \sum_{rs} \pi_{rs} \left(q_{rs}^{total} - \sum_k f_k^{rs} - q_{rs}^t \right) \tag{22}$$

Take the derivative to the route flow f_k^{rs},

$$\frac{\partial L(f_k^{rs}, q_{rs}^t, \pi_{rs})}{\partial f_k^{rs}} = c_k^{rs} + \frac{1}{\theta_K} (\ln f_k^{rs} + 1) - \frac{1}{\theta_K} \left(\ln \sum_l f_l^{rs} + 1 \right) - \pi_{rs} = 0, \forall k, r, s$$

$$\frac{1}{\theta_K} \ln \frac{f_k^{rs}}{\sum_l f_l^{rs}} = \pi_{rs} - c_k^{rs}$$

$$\frac{f_k^{rs}}{\sum_l f_l^{rs}} = \exp\{\theta_K (\pi_{rs} - c_k^{rs})\}$$

$$1 = \sum_l \exp\{\theta_K (\pi_{rs} - c_l^{rs})\} \tag{23}$$

Thus,

$$1 = \exp(\theta_K \pi_{rs}) \sum_l \exp\{-\theta_K c_l^{rs}\} \tag{24}$$

By rearranging,

$$w_{rs}^{car} = \pi_{rs} = -\frac{1}{\theta_K} \ln \sum_l \exp\{-\theta_K c_l^{rs}\}. \tag{25}$$

□

Note that π_{rs} is the EPC from r to s.

(2) Shared Network. Different travel modes may not operate on independent physical networks, such as the regular bus and car. In such a case, the multiple modes share the same physical network. The effect of sharing the same facilities will certainly influence the flow pattern of the maximum total demand. Here, we consider the modes of bus and car, which share the same road network. The travel demand for the two modes can be converted to the standard unit of the traffic flow, i.e., passenger car unit. Therefore, the following formulation is conducted.

$$\min_{(f_k^{rs}, q_{rs}^m)} \sum_a \int_0^{v_a} t_a(x)dx - \sum_{rs} \sum_{m=1}^{2} \Psi_{rs}^m q_{rs}^m + \frac{1}{\theta_M} \sum_{rs} \sum_{m=1}^{2} q_{rs}^m \ln q_{rs}^m + \frac{1}{\theta_K} \sum_{rs} \sum_{m=1}^{2} \sum_k f_{mk}^{rs} \ln f_{mk}^{rs} - \frac{1}{\theta_K} \sum_{rs} \sum_{m=1}^{2} q_{rs}^m \ln q_{rs}^m, \tag{26}$$

$$s.t. \sum_m q_{rs}^m = q_{rs}^{total}, \forall r \in R, s \in S, \tag{27}$$

$$\sum_k f_{mk}^{rs} = q_{rs}^m, \forall m \in M_{rs}, \forall r \in R, s \in S, \tag{28}$$

$$v_a = \sum_m \frac{PCE_m}{OCC_m} \sum_{rs} \sum_k f_{mk}^{rs} \delta_{a,mk}^{rs}, \forall a \in A, \tag{29}$$

$$\mu \bullet \bar{q}_{rs} = q_{rs}^{total}, \forall r \in R, s \in S, \tag{30}$$

$$f_{mk}^{rs} \ge 0, \forall k \in K_{rs}, m \in M_{rs}, r \in R, s \in S, \tag{31}$$

where PCE_m is the passenger car equivalent (PCE) factor of mode m. OCC_m is the average occupancy of mode m, which is calculated as the average number of persons occupying a vehicle of mode m. Note that, in the above formulation, the link travel times of bus and car are assumed to be the same. In Eq. (29), v_a denotes the traffic flow by integrating the car and bus flows, counted in *passenger unit car*. In the bimodal model for shared network, the third term of the objective function is associated with the entropy maximization of mode choices, which can be easily derived as the route choice entropy in Remark 1. The fourth and fifth terms are associated with the entropy maximization of route choices.

In the next stage, we incorporate the nested tree structure of the NL model in the mode choice level to formulate the proposed NL-PSL model, in which the PSL uses a path-size factor to deal with the route overlapping problem (or route similarity). For each formulation, the network capacity problem will be resolved and discussed in the numerical section, and thus the advantages of the nested structure for multimodal transportation network will be shown.

2.2.3. CMSTA Model for Multimodal Network. In this subsection, the bimodal demand model will be generalized to the multimodal case firstly, in which the multimodal interaction and route overlapping issues are considered. Then, the mode similarity issue will be handled by adopting a two-level nested structure in mode choice.

(1) MNL Structure with Route Overlapping Consideration. The derivation of the multimodal demand model is ready by following the formulation of the bimodal demand model for the shared network. Only need to change the upper limit from 2 to |M| (the number of modes) in the summation of the O-D demand by modes. Nevertheless, considering the independently distributed assumption, i.e., route overlapping problem, imposed on the logit-based SUE model, we introduce a path-size factor ϖ_k^{rs} to correct the EPC of the overlapped routes. The path-size factor $\varpi_k^{rs} \in (0, 1]$ is defined for each route k and is decided according to the length of links within a route and the relative lengths of routes that share a link. A typical form is as follows [32]:

$$\varpi_k^{rs} = \sum_{a \in \Gamma_k} \frac{l_a}{L_k^{rs}} \frac{1}{\sum_{l \in K_{rs}} \delta_{al}^{rs}}, \forall k \in K_{rs}, r \in R, s \in S, \tag{32}$$

where l_a is the length of link a, L_k^{rs} is the length of route r connecting O-D pair rs, Γ_k is the set of all links in route r between O-D pair (r, s), and δ_{al}^{rs} is equal to 1 for link a on route r between O-D pair (r, s) and 0 otherwise. Hence, the combined multimodal demand model can be formulated as

$$\begin{aligned} \min_{(f_k^{rs}, q_{rs}^m)} & \sum_a \int_0^{v_a} t_a(x)dx - \frac{1}{\theta_K} \sum_{rs} \sum_{mk} f_{mk}^{rs} \ln \varpi_k^{rs} - \sum_{rs} \sum_m \Psi_{rs}^m q_{rs}^m \\ & + \frac{1}{\theta_M} \sum_{rs} \sum_m q_{rs}^m \ln q_{rs}^m + \frac{1}{\theta_K} \sum_{rs} \sum_{mk} f_{mk}^{rs} \ln f_{mk}^{rs} \\ & - \frac{1}{\theta_K} \sum_{rs} \sum_m q_{rs}^m \ln q_{rs}^m. \end{aligned} \tag{33}$$

Equation (27)–(31).

In the combined multimodal model, the second term of the objective function is associated with the path-size factor. The third term is associated with modal attractiveness. The fourth term is for entropy maximization of mode choices. The last two terms are associated with the entropy maximization of route choices as we interpreted in Remark 1.

(2) Nested Structure for Handling Mode Similarity. This section extends the multimodal model with MNL to the formulation with a two-level structured NL [38]. With the nested structure, the travel modes with similarity (such as bus and metro are recognized as public transit) are modeled in the same nest, which allows considering the correlations of the similar modes. Consequently, the CMSTA model with NL is formulated as the following MP formulation.

$$\begin{aligned} \min_{(f_{umk}^{rs}, q_{rs}^{um})} & \sum_a \int_0^{v_a} t_a(x)dx - \frac{1}{\theta_K} \sum_{rs} \sum_{mk} f_{umk}^{rs} \ln \varpi_k^{rs} - \sum_{rs} \sum_{um} \Psi_{rs}^{um} \bullet q_{rs}^{um} \\ & + \frac{1}{\theta_U} \sum_{rs} \left(\sum_u \sum_m q_{rs}^{um} \ln \sum_n q_{rs}^{un} - \sum_{um} q_{rs}^{um} \ln \sum_{wn} q_{rs}^{wn} \right) \\ & + \frac{\theta_M}{\theta_U} \sum_{rs} \sum_u \left(\sum_m q_{rs}^{um} \ln q_{rs}^{um} - \sum_m q_{rs}^{um} \ln \sum_n q_{rs}^{un} \right) \\ & + \frac{1}{\theta_K} \sum_{rs} \sum_{um} \left(\sum_k f_{umk}^{rs} \ln f_{umk}^{rs} - \sum_k f_{umk}^{rs} \ln \sum_l f_{uml}^{rs} \right), \end{aligned} \tag{34}$$

$$\sum_{um} q_{rs}^{um} = q_{rs}^{total}, r \in R, s \in S, \tag{35}$$

$$\sum_k f_{umk}^{rs} = q_{rs}^{um}, \forall m \in M_{rs}^u, u \in U_{rs}, r \in R, s \in S, \tag{36}$$

$$v_a = \sum_{um} \frac{PCE_{um}}{OCC_{um}} \sum_{rs} \sum_k f_{umk}^{rs} \delta_{a,umk}^{rs}, \forall a \in A, \tag{37}$$

$$\mu \bullet \bar{q}_{rs} = q_{rs}^{total}, \tag{38}$$

$$f_{umk}^{rs} \geq 0, \forall k \in K_{rs}^{um}, m \in M_{rs}^u, u \in U_{rs}, r \in R, s \in S, \tag{39}$$

$$0 < q_{rs}^{um} \leq q_{rs}^{total}, \forall u \in U_{rs}, r \in R, s \in S, \tag{40}$$

where the label $u \in U_{rs}$ for the variables are the nest of the similar modes between (r, s). θ_U is the scale parameter for nest choice.

Proposition 2. *The MP formulation in Eqs. (34)–(40) gives the route choice solution of the PSL model and mode choice solution of the NL model.*

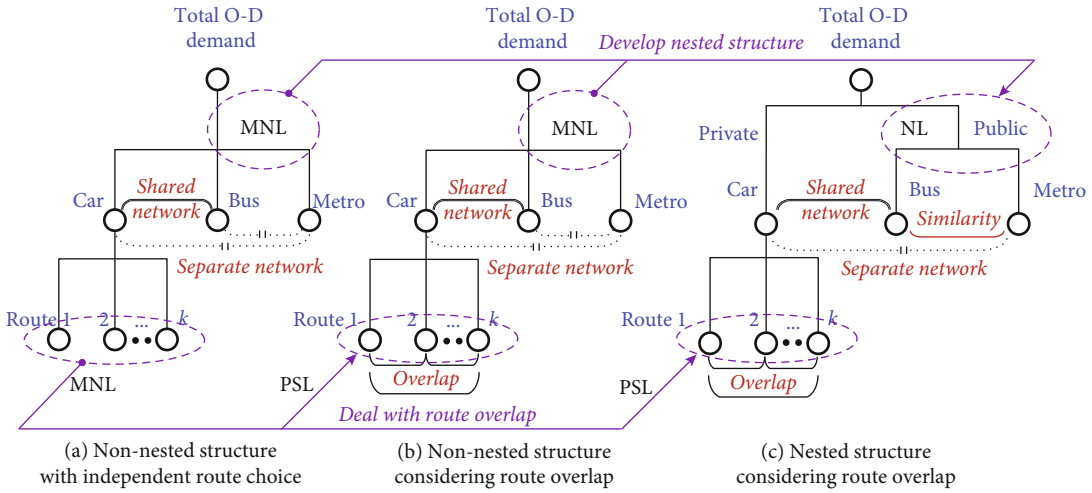

Figure 3: Structures for nonnested and nested multimodal models.

Step 0: *Initialization*. Obtain an initial flow pattern $\{f_{umk}^{rs,(0)}, q_{rs}^{um,(0)}\}$ using eqs. (46)-(53) based on the free-flow link travel time, and set n: =0.

Step 1: *Descent direction*. Update the network cost with the current flow pattern $\boldsymbol{X}^n = \{f_{umk}^{rs,(n)}, q_{rs}^{um,(n)}\}$. Find an auxiliary solution $\boldsymbol{Y}^n = \{\widehat{f}_{umk}^{rs,(n)}, \widehat{q}_{rs}^{um,(n)}\}$ using eqs. (46)-(53) with the updated network cost.

Step 2: *Determine step size*. Choose the step size as $\alpha^{(n)} = 1/\beta^{(n)}$, where $\beta^{(n)}$ is given by

$$\beta^{(n)} = \begin{cases} \beta^{(n-1)} + \lambda_1, \text{if} ||\boldsymbol{Y}^n - \boldsymbol{X}^n|| \geq ||\boldsymbol{Y}^{n-1} - \boldsymbol{X}^{n-1}|| \\ \beta^{(n-1)} + \lambda_2, \text{otherwise} \end{cases}$$

where $\lambda_1 > 1$ and $0 < \lambda_2 < 1$.

Step 3: *Updating solution*. $\boldsymbol{X}^{(n+1)} \coloneqq \boldsymbol{X}^{(n)} + \alpha^{(n)} \bullet (\boldsymbol{Y}^{(n)} - \boldsymbol{X}^{(n)})$.

Step 4: *Convergence criterion*. If the convergence criterion is satisfied, then stop; otherwise, return to step 1, and set $n \coloneqq n + 1$.

Algorithm 1: Solving the CMSTA model.

Proof. The Lagrange of the MP problem can be given by

$$\begin{aligned} L(f_{umk}^{rs}, q_{rs}^{um}, \pi_{um}^{rs}, \lambda_{rs}) &= \sum_a \int_0^{v_a} t_a(x)dx - \frac{1}{\theta_K} \sum_{rs} \sum_{mk} f_{umk}^{rs} \ln \varpi_k^{rs} \\ &- \sum_{rs} \sum_{um} \Psi_{rs}^{um} \bullet q_{rs}^{um} + \frac{1}{\theta_U} \sum_{rs} \left(\sum_u \sum_m q_{rs}^{um} \ln \sum_n q_{rs}^{un} - \sum_{um} q_{rs}^{um} \ln \sum_{wn} q_{rs}^{wn} \right) \\ &+ \frac{\theta_M}{\theta_U} \sum_{rs} \sum_u \left(\sum_m q_{rs}^{um} \ln q_{rs}^{um} - \sum_m q_{rs}^{um} \ln \sum_n q_{rs}^{un} \right) \\ &+ \frac{1}{\theta_K} \sum_{rs} \sum_{um} \left(\sum_k f_{umk}^{rs} \ln f_{umk}^{rs} - \sum_k f_{umk}^{rs} \ln \sum_l f_{uml}^{rs} \right) \\ &+ \sum_{rs} \lambda_{rs} \left(q_{rs}^{total} - \sum_{um} q_{rs}^{um} \right) + \sum_{rs} \sum_{um} \pi_{um}^{rs} \left(q_{rs}^{um} - \sum_k f_{umk}^{rs} \right) \end{aligned} \tag{41}$$

where $\lambda_{rs}, \pi_{um}^{rs}$ are, respectively, the dual variables associated with the constraints (35) and (36). Given the equilibrium condition holds at the optimal solution with only positive flow. The following KKT condition can be obtained. We assume that $PCE_{um}/OCC_{um} = 1, \forall m, u$. □

(1) Route choice

$$\begin{aligned} \frac{\partial L(f_{umk}^{rs}, q_{rs}^{um}, \lambda_{rs}, \pi_{um}^{rs})}{\partial f_{umk}^{rs}} &= c_{umk}^{rs} + \frac{1}{\theta_K} (\ln f_{umk}^{rs} + 1) - \frac{1}{\theta_K} \\ &\cdot \left(\ln \sum_l f_{uml}^{rs} + 1 \right) - \frac{1}{\theta_K} \ln \varpi_k^{rs} - \pi_{um}^{rs} = 0, \forall k, m, u, r, s. \end{aligned} \tag{42}$$

Rearranging

$$\frac{f_{umk}^{rs}}{\sum_l f_{uml}^{rs}} = \varpi_k^{rs} \exp \{\theta_K (\pi_{um}^{rs} - c_{umk}^{rs})\}, \tag{43}$$

$$1 = \sum_l \varpi_l^{rs} \exp \{\theta_K (\pi_{um}^{rs} - c_{uml}^{rs})\}, \tag{44}$$

$$\frac{f_{umk}^{rs}}{\sum_l f_{uml}^{rs}} = \frac{\varpi_k^{rs} \exp \{\theta_K (\pi_{um}^{rs} - c_{umk}^{rs})\}}{\sum_l \varpi_l^{rs} \exp \{\theta_K (\pi_{um}^{rs} - c_{uml}^{rs})\}} = \frac{\varpi_k^{rs} \exp \{\theta_K (-c_{umk}^{rs})\}}{\sum_l \varpi_l^{rs} \exp \{\theta_K (-c_{uml}^{rs})\}}. \tag{45}$$

Step 0: *Initialization*. Start from an initial value $\mu^{(0)}$. Let n: =0.
Step 1: *Solving the CMSTA model.* Given the multiplier $\mu^{(n)}$, solve the CMSTA model to obtain the equilibrium link flows $\{v_a^m\}$ and mode-specific OD demand $\{q_{rs}^m\}$.
Step 2: *Sensitivity analysis.* Obtain $\nabla_\mu v_a^m(\mu^{(n)})$ and $\nabla_\mu q_{rs}^m(\mu^{(n)})$ from the sensitivity analysis of the CMSTA model.
Step 3: *Local approximation.* Approximate the upper-level capacity constraints using the sensitivity results, and then solve the resulted linear programming to obtain an auxiliary multiplier $\widehat{\mu}^{(n)}$.
Step 4: *Updating the multiplier.* $\mu^{(n+1)} \coloneqq \mu^{(n)} + \alpha \bullet (\widehat{\mu}^{(n)} - \mu^{(n)})$, where α is a step size.
Step 5: *Convergence test*. If the convergence test is satisfied, then stop; otherwise, return to step 1, and set $n \coloneqq n + 1$.

Algorithm 2: The SAB algorithm for the reserve network capacity model.

Thus,

$$P_{k|m} = \frac{\varpi_k^{rs} \exp\{\theta_K(-c_{umk}^{rs})\}}{\sum_l \varpi_l^{rs} \exp\{\theta_K(-c_{uml}^{rs})\}}. \tag{46}$$

(2) Mode choice

$$\frac{\partial L(f_{umk}^{rs}, q_{rs}^{um}, \lambda_{rs}, \pi_{um}^{rs})}{\partial q_{rs}^{um}} = \frac{\theta_M}{\theta_U}(\ln q_{rs}^{um} + 1) + \frac{1-\theta_M}{\theta_U} \cdot \left(\ln \sum_n q_{rs}^{un} + 1\right) - \Psi_{rs}^{um} + \pi_{um}^{rs} - \lambda_{rs} = 0, \forall m, u, r, s. \tag{47}$$

Rearranging

$$q_{rs}^{um}\left(\sum_n q_{rs}^{un}\right)^{1-\theta_M/\theta_M} = \exp\left\{\frac{\theta_U}{\theta_M}\left(\lambda_{rs} + \Psi_{rs}^{um} - \pi_{um}^{rs} - \frac{1}{\theta_U}\right)\right\}. \tag{48}$$

Summing all m gives

$$\left(\sum_n q_{rs}^{un}\right)^{1/\theta_M} = \exp\left\{\frac{\theta_U}{\theta_M}\left(\lambda_{rs} - \frac{1}{\theta_U}\right)\right\}\sum_m \exp\left\{\frac{\theta_U}{\theta_M}(\Psi_{rs}^{um} - \pi_{um}^{rs})\right\}. \tag{49}$$

Thus,

$$\sum_n q_{rs}^{un} = \exp\{\theta_U \lambda_{rs} - 1\}\left(\sum_m \exp\left\{\frac{\theta_U}{\theta_M}(\Psi_{rs}^{um} - \pi_{um}^{rs})\right\}\right)^{\theta_M}. \tag{50}$$

Then, summing all u gives

$$\sum_u \sum_n q_{rs}^{un} = q_{rs} = \exp\{\theta_U \lambda_{rs} - 1\}\sum_u \left(\sum_m \exp\left\{\frac{\theta_U}{\theta_M}(\Psi_{rs}^{um} - \pi_{um}^{rs})\right\}\right)^{\theta_M}. \tag{51}$$

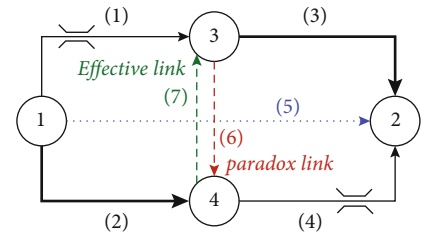

Figure 4: The Braess network for network capacity paradox.

Therefore, we have the marginal probability

$$\frac{\sum_n q_{rs}^{un}}{q_{rs}} = P_{u|rs} = \frac{(\sum_m \exp\{(\theta_U/\theta_M)(\Psi_{rs}^{um} - \pi_{um}^{rs})\})^{\theta_M}}{\sum_u (\sum_n \exp\{(\theta_U/\theta_M)(\Psi_{rs}^{un} - \pi_{un}^{rs})\})^{\theta_M}}. \tag{52}$$

And the conditional probability

$$\frac{q_{rs}^{um}}{\sum_n q_{rs}^{un}} = P_{m|u}^{rs} = \frac{\exp\{(\theta_U/\theta_M)(\Psi_{rs}^{um} - \pi_{um}^{rs})\}}{\sum_n \exp\{(\theta_U/\theta_M)(\Psi_{rs}^{un} - \pi_{un}^{rs})\}}. \tag{53}$$

Proposition 3. *The solution of NL-PSL model is unique.*

Proof. It is sufficient to prove that the objective function in Eq. (34) is strictly convex, as the feasible region is bounded by linear constraints only and is convex.

Note that the link travel time is assumed strictly increasing in term of the link flow. The Hessian matrix with respect to the route flow is obtained as

$$\frac{\partial^2 Z}{\partial f_{umk}^{rs} \partial f_{uml}^{rs}} = \begin{cases} \dfrac{\partial c_{umk}^{rs}}{\partial f_{umk}^{rs}} + \dfrac{1}{\theta_K}\left(\dfrac{1}{f_{umk}^{rs}} - \dfrac{1}{\sum_l f_{uml}^{rs}}\right) > 0, k = l \\ 0, k \neq l \end{cases}, \tag{54}$$

where $f_{umk}^{rs} \leq \sum_l f_{uml}^{rs}$, and thus the diagonal elements must be positive.

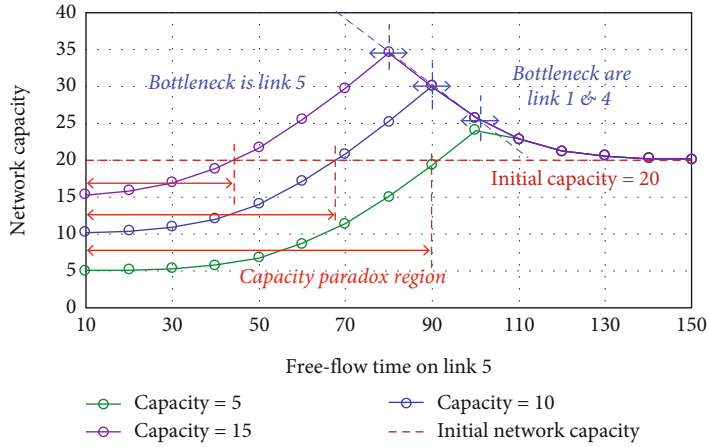

Figure 5: Network capacity with respect to the characteristics on the new added link.

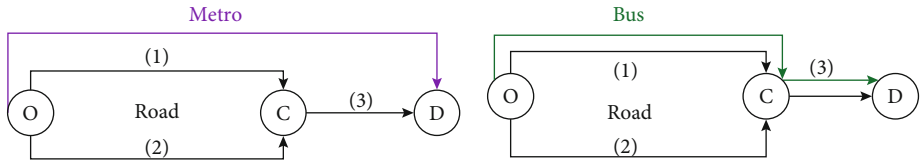

(a) construct a new metro line (b) operate a new bus service

Figure 6: Schemes of adding new mode to the road network.

The Hessian matrix with respect to the mode flow variables can be expressed as

$$\frac{\partial^2 Z}{\partial q_{rs}^{um}\partial q_{rs}^{un}} = \begin{cases} \dfrac{\theta_M}{\theta_U}\left(\dfrac{1}{q_{rs}^{um}} - \dfrac{1}{\sum_n q_{rs}^{un}}\right) + \dfrac{1}{\theta_U}\left(\dfrac{1}{\sum_n q_{rs}^{un}}\right) > 0, m = n \\ 0, k \neq l \end{cases}, \tag{55}$$

where $q_{rs}^{um} \leq \sum_n q_{rs}^{un}$, and thus the diagonal elements must be positive. Therefore, the above equations imply the positive definite Hessian matrix. Therefore, the NL-PSL model has a unique solution. This completes the proof. □

In summary, the multimodal network capacity model is formulated as bilevel programming, of which the upper-level model is given by Eqs. (1)–(3), and the lower-level model is given by Eqs. (34)–(40). Moreover, Figure 3 shows the process of developing the nested structure with route overlap correction based on the original MNL-based combined model. Not only that, the nested structure can be easily extended to consider intermodal travels (e.g., car and metro, bus and metro) by involving them as specified mode options. Also, the NL model can be regarded as a special case of the cross-nested logit model [38], and hence it is reasonable to extend the current nested structure to capture the mode similarity in different intermodal travelling stages [8].

3. Design of Solution Algorithm

The multimodal network capacity model is formulated as bilevel programming. Some early studies use the incremental assignment method by loading the travel demand gradually until the network capacity has been reached (e.g., [39]). Yang et al. [9] used an iterative estimation assignment algorithm to estimate the implicit relationship, referred to as *reaction function*, between the upper-level and lower-level decision variables. Chen and Kasikitwiwat [40] employed the genetic algorithm to solve the practical and ultimate network capacity problems in a small network. However, such approximate methods may not provide a good quality solution to the bilevel models, especially in real-size transportation networks [41]. On the other hand, the precision of the solution to the lower-level problem is important to locally evaluate the reaction function and further to the quality of the bilevel models [42]. Be aware of the aforementioned problems, this section will design an iterative solution algorithm, which is capable to solve the proposed multimodal network capacity model with good quality for practical purposes.

3.1. Solving the Lower Level Model. A key step of the SAB algorithm is solving the lower level equilibrium problem. For the multimodal network capacity model, the lower-level CMSTA problem is a NL-PSL-based stochastic equilibrium model in Eqs. (34)–(40). In this study, we use the self-regulated averaging (SRA) method [43] to solve the CMSTA model. The procedure is as follows.

3.2. Sensitivity Analysis of the CMSTA Model. The sensitivity analysis of the lower-level model is used to approximate the original nonlinear relationship, which transform the original bilevel programming to a single-level programming for simplifying its solution. A comprehensive review on the sensitivity analysis approaches for the transportation

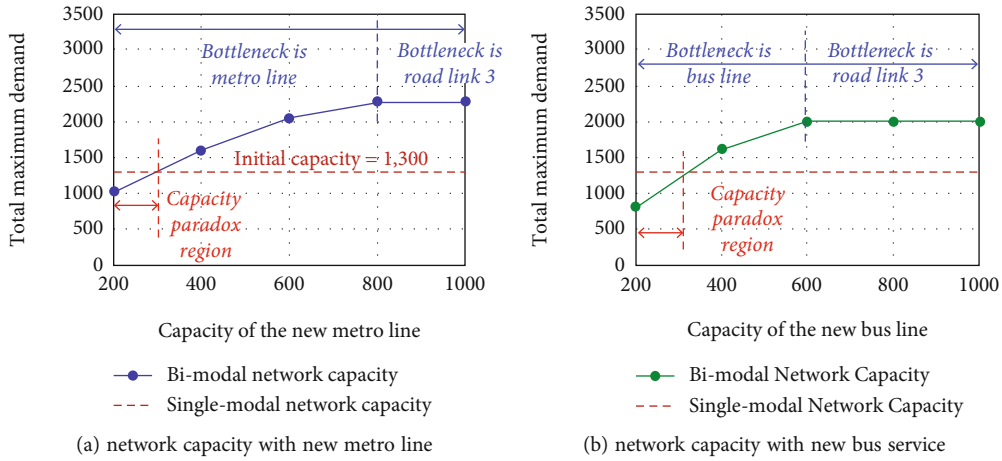

(a) network capacity with new metro line

(b) network capacity with new bus service

Figure 7: Effect on network capacity of adding new mode to road network.

equilibrium models can be referred to Du and Chen [44]. Since we have proved the solution of the NL-PSL-based CMSTA model is unique in the route flow space (i.e., Proposition 3), the analytical expressions can be obtained following the typical approach for the sensitivity analysis of the nonlinear programming by Fiacco [45].

Firstly, the Lagrange function of the CMSTA model with the O-D multiplier μ is as follows.

$$\begin{aligned} L(f_{umk}^{rs}, q_{rs}^{um}, \pi_{um}^{rs}, \lambda_{rs}, \mu) &= \sum_a \int_0^{v_a} t_a(x)dx + \frac{1}{\theta_K}\sum_{rs}\sum_{um}\left(\sum_k f_{umk}^{rs} \ln f_{umk}^{rs} - \sum_k f_{umk}^{rs} \ln \sum_l f_{uml}^{rs}\right) \\ &- \frac{1}{\theta_K}\sum_{rs}\sum_{mk} f_{umk}^{rs} \ln \bar{\omega}_k^{rs} + \sum_{rs}\sum_{um} \Psi_{rs}^{um} \bullet q_{rs}^{um} \\ &+ \frac{\theta_M}{\theta_U}\sum_{rs}\sum_u\left(\sum_m q_{rs}^{um} \ln q_{rs}^{um} - \sum_m q_{rs}^{um} \ln \sum_n q_{rs}^{un}\right) \\ &+ \frac{1}{\theta_U}\sum_{rs}\sum_u\sum_m q_{rs}^{um} \ln \sum_m q_{rs}^{um} + \sum_{rs}\sum_{um}\pi_{um}^{rs}\left(q_{rs}^{um} - \sum_k f_{umk}^{rs}\right) \\ &+ \sum_{rs}\lambda_{rs}\left(\mu \bullet \bar{q}_{rs} - \sum_{um} q_{rs}^{um}\right), \end{aligned} \tag{56}$$

where $\pi_{um}^{rs}, \lambda_{rs}$ are the Lagrangian multipliers. Thus, the first-order necessary conditions, i.e., the KKT conditions, of the CMSTA model are

$$\nabla_{f_{umk}^{rs}} L = c_{umk}^{rs} + \frac{1}{\theta_K}(\ln f_{umk}^{rs} + 1) - \frac{1}{\theta_K}\left(\ln \sum_l f_{uml}^{rs} + 1\right) - \frac{1}{\theta_K} \ln \bar{\omega}_k^{rs} - \pi_{um}^{rs} = 0, \forall k, m, u, r, s$$

$$\nabla_{q_{rs}^{um}} L = \frac{\theta_M}{\theta_U}(\ln q_{rs}^{um} + 1) + \frac{1-\theta_M}{\theta_U}\left(\ln \sum_n q_{rs}^{un} + 1\right) - \Psi_{rs}^{um} + \pi_{um}^{rs} - \lambda_{rs} = 0, \forall m, u, r, s$$

$$\nabla_{\pi_{um}^{rs}} L = q_{rs}^{um} - \sum_k f_{umk}^{rs} = 0, \forall m, u, r, s$$

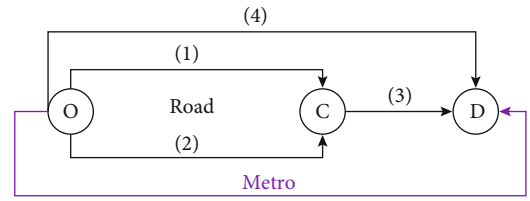

Figure 8: A bimodal network

$$\nabla_{\lambda_{rs}} L = \mu \bullet \bar{q}_{rs} - \sum_{um} q_{rs}^{um} = 0, \forall r, s, \tag{57}$$

where ∇ is the gradient operator. Let $M(\varepsilon)$ and $N(\varepsilon)$ be the Jacobians of the above system equations, we have

$$\mathrm{M}(\varepsilon) = \begin{bmatrix} \nabla^2_{f_{umk}^{rs}} L & O & -\Gamma^{\mathrm{T}} & O \\ O & \nabla^2_{q_{rs}^{um}} L & \mathrm{I} & -\Phi^{\mathrm{T}} \\ -\Gamma & I & O & O \\ O & -\Phi & O & O \end{bmatrix}, \tag{58}$$

$$\mathrm{N}(\varepsilon) = [OOO\mathrm{I}]^T,$$

where $\nabla^2_{f_{umk}^{rs}} L = (\partial c_{umk}^{rs}/\partial f_{umk}^{rs}) + (1/\theta_K)(1/f_{umk}^{rs} - 1/\sum_l f_{uml}^{rs})$, $\nabla^2_{q_{rs}^{um}} L = (\theta_M/\theta_U)(1/q_{rs}^{um} - 1/\sum_n q_{rs}^{un}) + (1/\theta_U)(1/\sum_n q_{rs}^{un})$, and ∇^2 is the second-order gradient operator. Γ denotes the route/O-D incidence matrix; Φ denotes the mode/O-D incidence matrix; I is the identity matrix. Because the Hessian of the CMSTA model is positive definite (as the proof of proposition 3) and the incidence matrices of Ψ, Φ, and I are linearly row independent, the Jacobian matrix $M(\varepsilon)$ should be invertible. Thereby, the derivatives of the input variables to the perturbed parameters are given by

$$\begin{bmatrix} \nabla_\mu f_{umk}^{rs} \\ \nabla_\mu q_{rs}^{um} \\ \nabla_\mu \pi_{um}^{rs} \\ \nabla_\mu \lambda_{rs} \end{bmatrix} = [\mathrm{M}(\varepsilon)]^{-1}[-\mathrm{N}(\varepsilon)]. \tag{59}$$

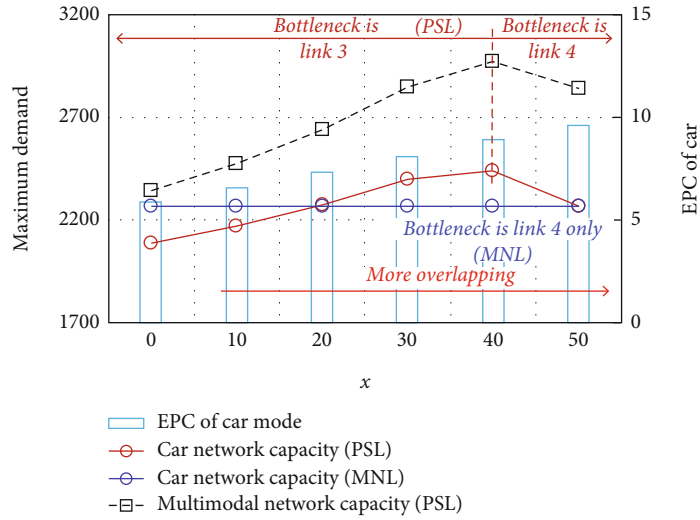

Figure 9: Effect of route overlapping on network capacity.

Then, the derivatives of link flows are calculated by $\nabla_\mu v_a = \Delta^T \bullet \text{diag}\,(PCE_{um}/OCC_{um}) \bullet \nabla_\mu f^{rs}_{umk}$, where Δ is the link/route incidence matrix.

3.3. Solving the Network Capacity Problem with a Bilevel Framework. The SAB algorithm falls into the category of the decent method, and has been widely used for solving the bilevel programming with an equilibrium assignment in the lower-level problem [9, 46]. Utilizing the sensitivity analysis results, the nonlinear constraints in the upper-level model is approximated as:

$$v_a^m\left(\mu^{(n)}\right) + \nabla_\mu v_a^m\left(\mu^{(n)}\right) \bullet \left(\mu - \mu^{(n)}\right) \le \varphi_a^m C_a^m, \forall a \in A, m \in M,$$
$$q_{rs}^m\left(\mu^{(n)}\right) + \nabla_\mu q_{rs}^m\left(\mu^{(n)}\right) \bullet \left(\mu - \mu^{(n)}\right) \le Q_{rs}^m, \forall m \in M, r \in R, s \in S, \quad (60)$$

where $\nabla_\mu v_a^m(\mu^{(n)})$ and $\nabla_\mu q_{rs}^m(\mu^{(n)})$ obtained from the sensitivity analysis of the CMSTA model. Thus, the sensitivity analysis-based algorithm is summarized as follows.

4. Numerical Examples

In this section, we provide three detailed examples to illustrate: (i) the effect of adding new link and (ii) the effect of adding a new mode to the network capacity; (iii) the effect of route overlap and mode similarity to the network capacity. After that, a multimodal transportation system is drawn from a real urban area. The capacities of the multimodal network are evaluated under scenarios with different network improvement measures, which demonstrate the effective ways of increasing network capacity for multimodal transportation systems.

4.1. Effect of Adding New Link. Consider the road network in Figure 4, which has been used to illustrate the Braess paradox and then been adopted for network capacity paradox [6]. In this study, we retain the link characteristics and performance functions from Yang and Bell [6]. In the original network before the new link is added, the link cost functions are: $t_1(v_1) = 20 + 2v_1$, $t_2(v_2) = 50 + v_2$, $t_3(v_3) = 50 + v_3$, and $t_4(v_4) = 20 + 2v_4$. The link capacities are $C_1 = C_4 = 10$ and $C_2 = C_3 = 20$. It is not hard to find link 1 and link 4 are the bottlenecks in the original network. The maximum demand can be sent from node 1 to node 2 is bound by the capacities of link 1 and 4. Since the conditions for the two routes $(1 \longrightarrow 3 \longrightarrow 2;\ 1 \longrightarrow 4 \longrightarrow 2)$ are the same, the capacity of this network is 20. To promote the capacity of this network, there are three options to add a new link in the network: link 5, link 6, or link 7, as Figure 4 shows. Obviously, in any case, the route diversity can be increased as a new route will be introduced in the expanded network.

It has been verified in Yang and Bell [6], adding link 6 will certainly result in a decrease in total network capacity. Hence, link 6 is regarded as the paradox link for this network. On the contrary, adding link 7 generally can increase the network capacity. In this study, we consider the option of adding link 5 (from node 1 to node 2). The cost function of the new link is given by $t_5(v_5) = t_5^0 + v_5$. The capacity of the new added link 5 is assumed to be 5, 10, and 15. For each level of link capacity, the free-flow travel time on link 5 (i.e., t_5^0) varies from 10 to 150. The capacity of the expanded network is calculated with respect to different combinations of link capacity and free-flow time, and the results are illustrated in Figure 5. For the SUE model, we set $\theta_K = 0.1$.

From Figure 5, the new link 5 may not always promote the total network capacity. When the free-flow time on link 5 is low, more travel demand will transfer from the original two routes $(1 \longrightarrow 3 \longrightarrow 2;\ 1 \longrightarrow 4 \longrightarrow 2)$ to the new route $(1 \longrightarrow 2)$. In this situation, link 5 should have sufficient capacity to allocate the new attracted demand. As Figure 5 shows, if the capacity of link 5 is insufficient to deal with the transferred demand, the expanded network could have a lower capacity than the original one, which results in the paradox phenomenon. In this case, the bottleneck will shift

from link 1 and 4 to link 5. From the administrators' aspect, if a new parallel link is planned to be constructed between the OD pair, it should have enough capacity, and not have very short travel time which could share too much travel demand and create a new bottleneck.

4.2. Effect of Adding Mode Choice Alternative. Figure 6 is a road network with only one OD pair (from node O to node D). The travel time functions of the three (road) links are given by: $t_1 = 10 + 2(v_1/C_1)$, $t_2 = 10 + 2(v_2/C_2)$, and $t_3 = 5 + (v_3/C_3)$. The parameters for travel choices are assumed as $\theta_K = 1.0, \theta_M = 0.5$. The link capacities are assumed as 800, 800, and 1,300, respectively. It is easy to identify if the network capacity is 1,300 from O to D, bound by the capacity of link 3. If the administrator wants to promote the systematic transport capacity by adding a new travel mode, the metro and bus can be two usual options. As Figure 6(a), to add the metro to the transportation system, a separate new line should be constructed physically independent to the road network. As Figure 6(b), to add bus service, the existing road network can be utilized by sharing links with passenger cars. Also, we assume the PCE factor, PCE_m, is set to 2.5 for bus, and 1 for passenger car. The average occupancy, OCC_m, is set to 25 for bus, and 1.2 for passenger car. The attractiveness of the car, bus, and metro are set to 0, -3.5, and -1.5, respectively, which assumes driving is more preferred in this area. Also, the travel cost of the metro is assumed to be a constant, and here let $w_{rs}^{metro} = 15$.

To show how adding new mode influences the systematic capacity, we consider that the capacity of the new metro line changes from 200 to 1,000; for the bus service, we assume the new bus line travels through links 1 and 2, and its capacity is changed 200 to 1,000 as well. The results of network capacity are illustrated in Figure 7. In both cases, the total travel demand is firstly restricted by new modes and then bound by link 3 of the road network. Same as experiences, adding a new metro line can expand the total network capacity more compared with adding a new bus service. One intuitive reason is that the metro usually owns independent network facilities and has a larger transportation ability. Another persuasive reason is the EPC of the metro is lower than that of the bus because the bus's travel time depends on road congestion. In addition, Figure 7 also shows the capacity paradox region for both cases, in which the capacity of the new mode is too low. In this situation, adding new mode could reduce the systematic capacity because queues will form in the new mode.

Remark 2. From the experiments in Section 4.1 and 4.2, we note that either adding a new link or adding a new mode could lead to a paradox phenomenon on network capacity. This usually occurs when the new link or mode creates a better travel option (e.g., route or mode) but cannot provide sufficient capacity at the same time. In practice, the capacity paradox more usually occurs when adding new links, because the newly added mode normally has sufficient capacity to allocate the new attracted demand. In both cases, it is necessary to avoid the occurrence of capacity paradox, especially in network design problems. An efficient way is to maximize the network reserve capacity in network design problems [6].

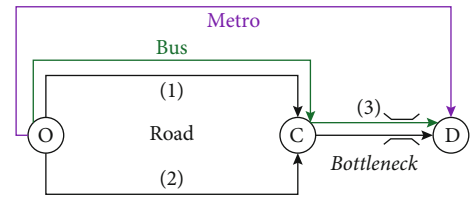

Figure 10: A network with three travel modes.

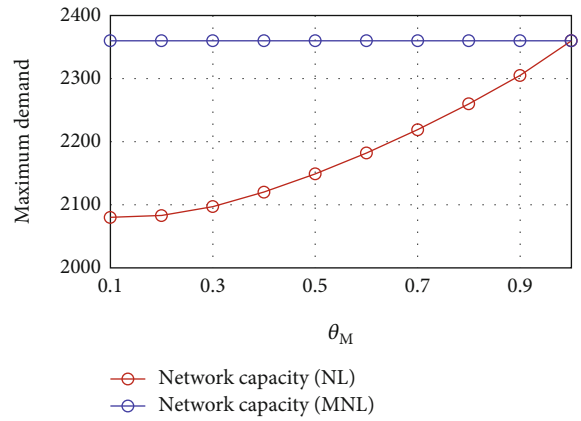

Figure 11: Effect of mode similarity on network capacity.

4.3. Effect of Route Overlapping and Mode Similarity. This section shows how considering route overlap and mode similarity will affect the network capacity evaluation. The multimodal network capacity is evaluated to demonstrate: (1) the effect of route overlapping; (2) the effect of mode similarity; and (3) the effect of considering both.

The first experiment in this section is conducted on a bimodal network in Figure 8. For the road network, there are three routes connecting the only OD pair (from node O to node D). Clearly, the two lower routes are overlapping on link 3. We assume the length of the overlapping portion to be x. Thus, the link cost functions are: $t_1(v_1) = (50 - x) + 2(v_1/C_1)$, $t_2(v_2) = (50 - x) + 2(v_2/C_2)$, $t_3(v_3) = x + (v_3/C_4)$, and $t_4(v_4) = 55 + (v_4/C_4)$. Also, the capacities of the road links are $C_1 = C_2 = C_3 = C_4 = 10$. A metro line also exists from O to D, and its travel cost and attractiveness are set to be 60 and -1.5, respectively. The parameters for mode choice and route choice are assumed as $\theta_K = 0.1$, $\theta_M = 0.2$.

In this example, the path-size factors of the three routes are 1, (100 − x)/100 and (100 − x)/100. By increasing x from 0 to 50, the capacity of road network and bimodal system are evaluated and presented in Figure 9. For comparison, the network capacities are evaluated by using the MNL model, which does not consider the overlapping issue. Also, the EPC of the car mode can be obtained under different level of overlapping. The EPC of car mode with PSL model is shown in Figure 9. The EPC of car mode can be derived

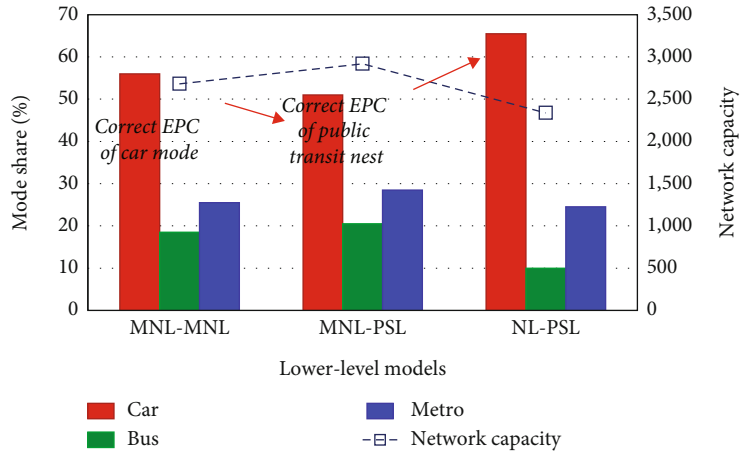

Figure 12: Results of network capacity with different lower-level models.

using Eq. (44), and is given by $w_{rs}^{car} = -(1/\theta_K) \ln \sum_l \varpi_k^{rs} \exp\{-\theta_K c_l^{rs}\}$.

Figure 9 indicates that the route overlapping issue has significant influences on the evaluation of road network capacity. Moreover, considering overlapping issue could change the EPC of the car mode, and further affect the capacity results for the entire bimodal system. Besides, regarding the overlapping degree, the bottleneck at maximum demand will change from link 3 to link 4 in this example. However, when employing the MNL model, the network capacity results have nothing to do with the route overlapping.

The second example demonstrates the effect of mode similarity on the multimodal network capacity. The multimodal network with the car, bus and metro mode is shown as Figure 10. There is only one OD pair from O to D. The bus mode is assumed to share the road network with car mode. In this example, the network characteristics are set the same as Section 4.2. The capacities of the two public transit modes are assumed sufficient large. To show the impact of mode similarity, the NL and MNL are employed for the mode choice in this example. For route choice, the dispersion parameter is set as $\theta_K = 0.7$. For MNL the parameters for choosing mode is set as $\theta'_M = 0.7$. For NL, the parameters for choosing nests are assumed as $\theta_U = 0.7$, while the parameters for choosing modes in each nest, θ_M, is varied from 0.1 to 0.9. As we know, a smaller value of θ_M for NL indicates a higher mode similarity; otherwise, at $\theta_M = 1$, the NL model produces the same results as the MNL model, which means the mode similarity is not considered. From Figure 11, considering mode similarity will produce different network capacity results. As the bottleneck for this example network is at road link 3, along with the increase of similarity for public transit modes, more travel demand transfers to the car mode and results in a lower capacity of the multimodal network.

The third example shows how considering route overlap and mode similarity will affect the mode share and further impact the evaluation of network capacity. We again employ the combination of all three modes in Figure 10. The setting values of the parameters are same, except that the mode choice parameter in each nest, θ_M, is fixed at 0.5. The multimodal network capacity is evaluated under three formulations: (1) with the MNL-MNL model (without considering route overlap and mode similarity), (2) with the MNL-PSL model (only dealing with route overlap), and (3) with the NL-PSL model (dealing with both route overlap and mode similarity). The results are shown in Figure 12.

Figure 12 demonstrates the effect of route overlap and mode similarity to the total network capacity and the share rate of three travel modes. From the MNL-MNL to the MNL-PSL model, by which the route overlapping problem is tackled, the EPC of car mode is corrected by the path-size factor of PSL. It results in the EPC of car increasing, and thus the travel demand transfers from the car mode to the other two modes. As there is much spare capacity of the bus and metro lines, more total travel demand can be raised until the road network reaches saturation again. Therefore, the network capacity evaluated by using the MNL-PSL is larger than that by the MNL-MNL. Furthermore, from the MNL-PSL to the NL-PSL model, the mode similarity is modeled by NL. The nest structure enlarges the EPC of the travel modes from the same nest by considering the correlations. It results in the travel demand shifting from the public transit modes back to the car mode. Thus, the crowdedness in the road network is increased, and then the whole system reaches its capacity with a lower level of total demand since the constraints from the road network. Without considering the mode similarity, the network capacity could be overestimated. Note that considering both route overlap and mode similarity may not necessary to increase the network capacity result.

4.4. A Case Study. This section conducts a case study based on a real multimodal transportation network, as shown in Figure 13. Four scenarios (including the base scenario) are designed to discuss: (1) how building a new road segment affects the network capacity; (2) how improving public transport attractiveness benefit to the total network capacity of the urban transportation system; and (3) how much the network capacity will be improved by constructing a new metro line.

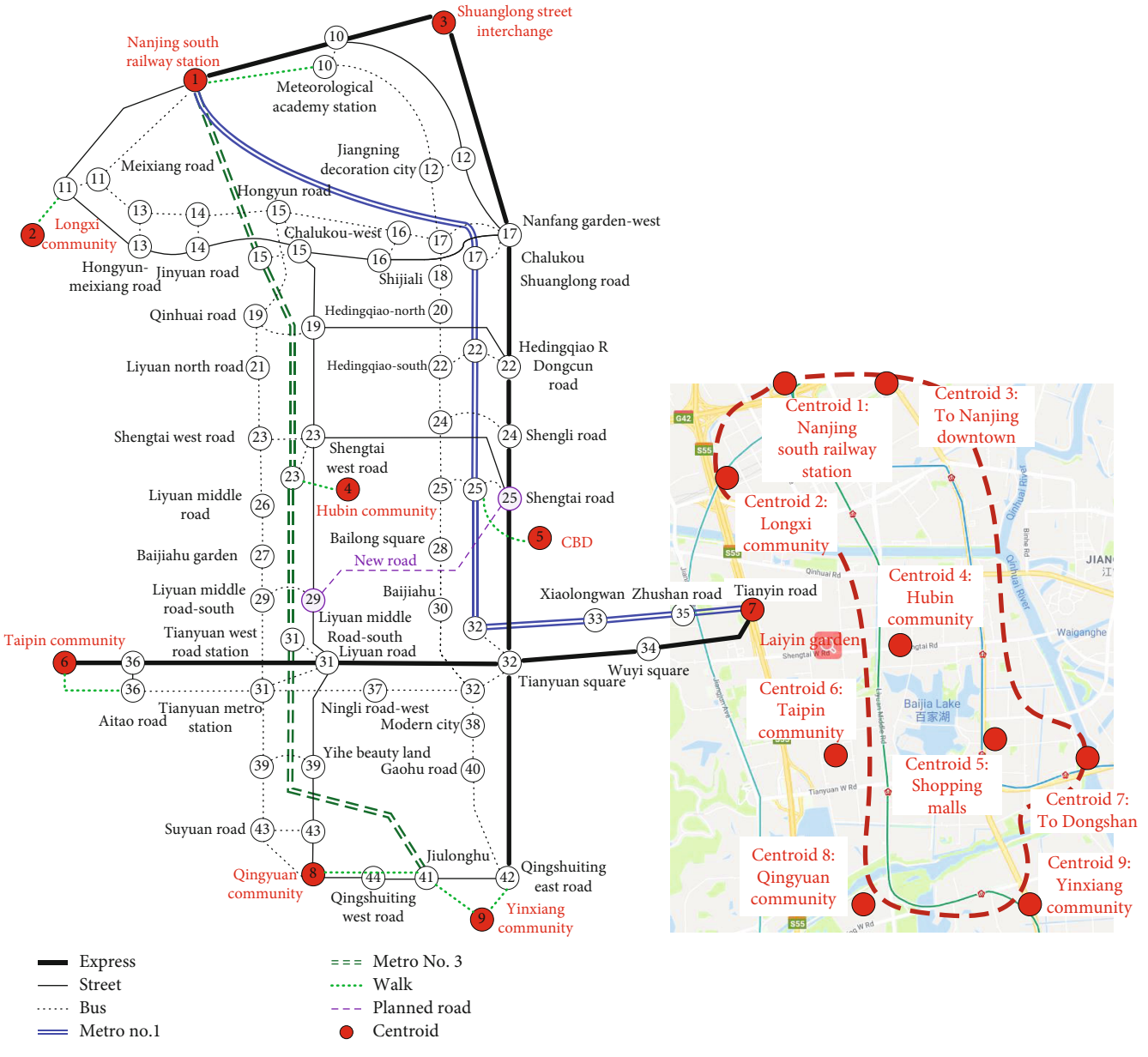

Figure 13: A multimodal network from Jiangning District in Nanjing.

Table 1: Total OD demand of the multimodal system in Figure 13.

O\D	1	2	3	4	5	6	7	8	9
1	—	400	600	600	800	200	600	400	400
2	600	—	600	400	200	200	200	200	200
3	1200	600	—	400	400	600	800	200	600
4	600	400	400	—	1000	200	400	400	400
5	600	400	800	1000	—	800	1000	200	800
6	400	200	600	200	800	—	1000	200	400
7	400	200	200	200	1200	600	—	200	200
8	400	200	200	400	400	200	200	—	80
9	400	200	200	200	800	400	400	80	—

Table 2: Scenarios for evaluating network capacity.

Scenario	Description	Setting
0 base scenario	Evaluate network capacity before the improvement measures	$\Psi_{rs}^{bus} = -5, \Psi_{rs}^{metro} = -2.$
1 effect of adding new links	To show adding new links may cause the capacity paradox although the route diversity is increased	$\Psi_{rs}^{bus} = -5, \Psi_{rs}^{metro} = -2;$ Add new links (25, 29) and (29, 25)
2 effect of improving bus attractiveness	To show encouraging public transport priority could increase the multimodal network capacity	$\Psi_{rs}^{bus} = 0, \Psi_{rs}^{metro} = -2.$
3 effect of constructing a new metro line	To show the effectiveness of the new metro line on the enhancement of both network capacity and mode diversity	$\Psi_{rs}^{bus} = -5, \Psi_{rs}^{metro} = -2;$ Construct the metro line no. 3.

Table 3: Mode choice options between OD pairs.

O\D	1	2	3	4	5	6	7	8	9
1	—	B C	C	B C	B C M	B C	C M	B C	B C
2	B C	—	C	B C	B C	B C	C	B C	B C
3	C	C	—	C	C	C	C	C	C
4	B C	B C	C	—	C	B C	C	B C	B C
5	B C M	B C	C	C	—	B C	C M	B C	B C
6	B C	B C	C	B C	B C	—	C	B C	B C
7	C M	C	C	C	C M	C	—	C	C
8	B C	B C	C	B C	B C	B C	C	—	B C
9	B C	B C	C	B C	B C	B C	C	B C	—

Abbreviations: C, car; B, bus; M, Metro.

Figure 13 presents a multimodal transportation network in Jiangning District in Nanjing, China. In this network, 9 major centroids are identified, which are associated with 72 OD pairs. Table 1 lists the OD demand of these OD pairs. For demonstration, we consider the base scenario when only metro line No. 1 was built. Consider that the administrators want to improve the multimodal system to cope with the rapid-growing travel demand in this area. The network capacity will be of particular concern. Hence, the multimodal network capacities are calculated for several network improvement measures to find out how to increase the capacity of the multimodal system. The scenarios for evaluating multimodal network capacity are described in Table 2. We assume that the parameters of the CMSTA model are $\theta_U = 0.1, \theta_M = 0.5$, and $\theta_K = 0.2$.

4.4.1. Scenario 0. In the base scenario, the multimodal network capacity is evaluated by the MNL-MNL model and the NL-PSL model, respectively. The attractiveness of bus and metro are, respectively, set to be -5 and -2. A working route set with 183 routes is provided. Without considering the route overlapping and mode similarity, the reserve capacity produced by the MNL-MNL model is $\mu = 1.44$. On the contrary, by using the NL-PSL model, we obtain the corrected reserve network capacity as $\mu = 1.48$. Also, the congestion is identified at the road links (8, 43), (11, 1), (23, 29), (25, 32), (29, 31), (39, 31), and (43, 39) (where the volume/capacity ratios are over 0.95). The bottleneck is link (25, 32) in this case. Besides, the mode alternative is evaluated by counting the reasonable mode options between each OD pair. The mode choice options between OD pairs are listed in Table 3.

4.4.2. Scenario 1. As the road congestion at the maximum flow situation is identified at the links around node 25 and node 29, it is intuitive to enhance the network connection and supply in this area. From this point, one may suggest building a new road segment between node 25 and node 29. By applying this scheme, two new links are created, i.e., link (25, 29) and link (29, 25), with the same configuration. Let the free-flow time and capacity of the two new links be $t_0 = 4$ min and $C_a = 2{,}700\, pcu/hour$. From the computational results, we find that the total network capacity (denoted by μ) is declined, from 1.48 to 1.27. After bulding the new link, the bottlenecks of the network capacity are link (29, 31) and (31, 29). Figure 14 shows the maximum traffic flow patterns on the road network before and after adding the new link. The red links indicate high utilization of the link capacities, while the green links mean low utilization of the capacities. Thus, fewer links with high utilization can be observed. Figure 15 shows an aggregate view of the V/C ratios for all road links. The link V/C ratios are arranged from high to low. We note that with the new links, the overall V/C ratio declines in the road network, which shows an obvious reduction in the utilization of the network. The upper right region of Figure 15 indicates the network spare capacity which has not been utilized when the travel demand is maximized. Apparently, the proportion of this region reflects how much residual space has not

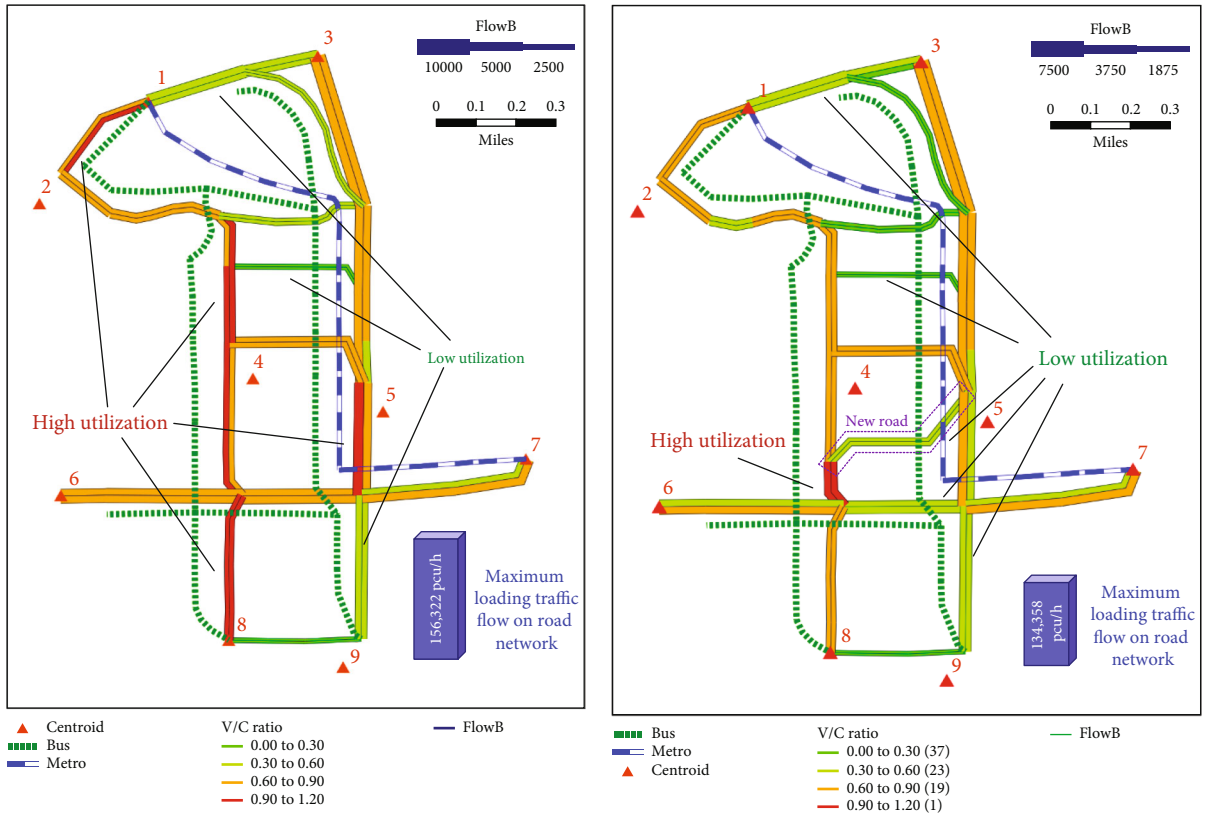

(a) before building the new link

(b) after building the new link

Figure 14: Maximum flow pattern on road network.

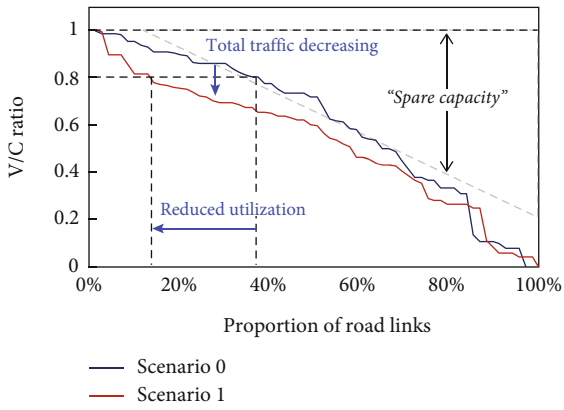

Figure 15: Change on road network utilization before and after adding new link.

been used when the total travel demand reaching the network capacity. Note that the network utilization is directly converted to the maximum demand. It is because the one trip may traverse many links along the route, so the total link flow may include duplicate counting of the travel trips. Besides, this result again verifies the conclusion in section 4.1, which shows adding new links may cause the capacity paradox in practice.

4.4.3. Scenario 2. Another option to increase the network capacity is to encourage the policy of public transport priority. This can be reflected as the increase in the attractiveness of bus or metro mode. In this scenario, we simply raise the attractiveness of the bus mode from -5 to 0. The rising of bus attractiveness could be realized by improving riding comfort, reducing bus fares, as well as raising people's awareness of "green travel", etc. From the result, the network capacity under public transport priority is increased significantly, from $\mu = 1.48$ to 1.58. It is because that increasing bus attractiveness can reduce the net travel impendence of the bus mode, and thus more travel demand will transfer from other modes (mainly from car mode) to buses. The bus share rate increases from 14.82% to 19.0%. Since the occupancy of buses is much higher than private cars, the traffic flow can be significantly declined on the road network with the same amount of trip demand. Hence, the total network capacity will be raised. The changes on the bus attractiveness, mode share, total capacity, and maximum flow pattern are illustrated in Figure 16. The result is consistent with the concept of the multimodal network capacity in Figure 1. Therefore, encouraging public transport priority usually improves the network capacity of the multimodal transportation systems.

4.4.4. Scenario 3. If the budget is enough, an effective way of enhancing the network capacity is to construct a new metro line in this area. In reality, the metro line No. 3 was constructed in Jiangning District after 2015. Here, we assumed

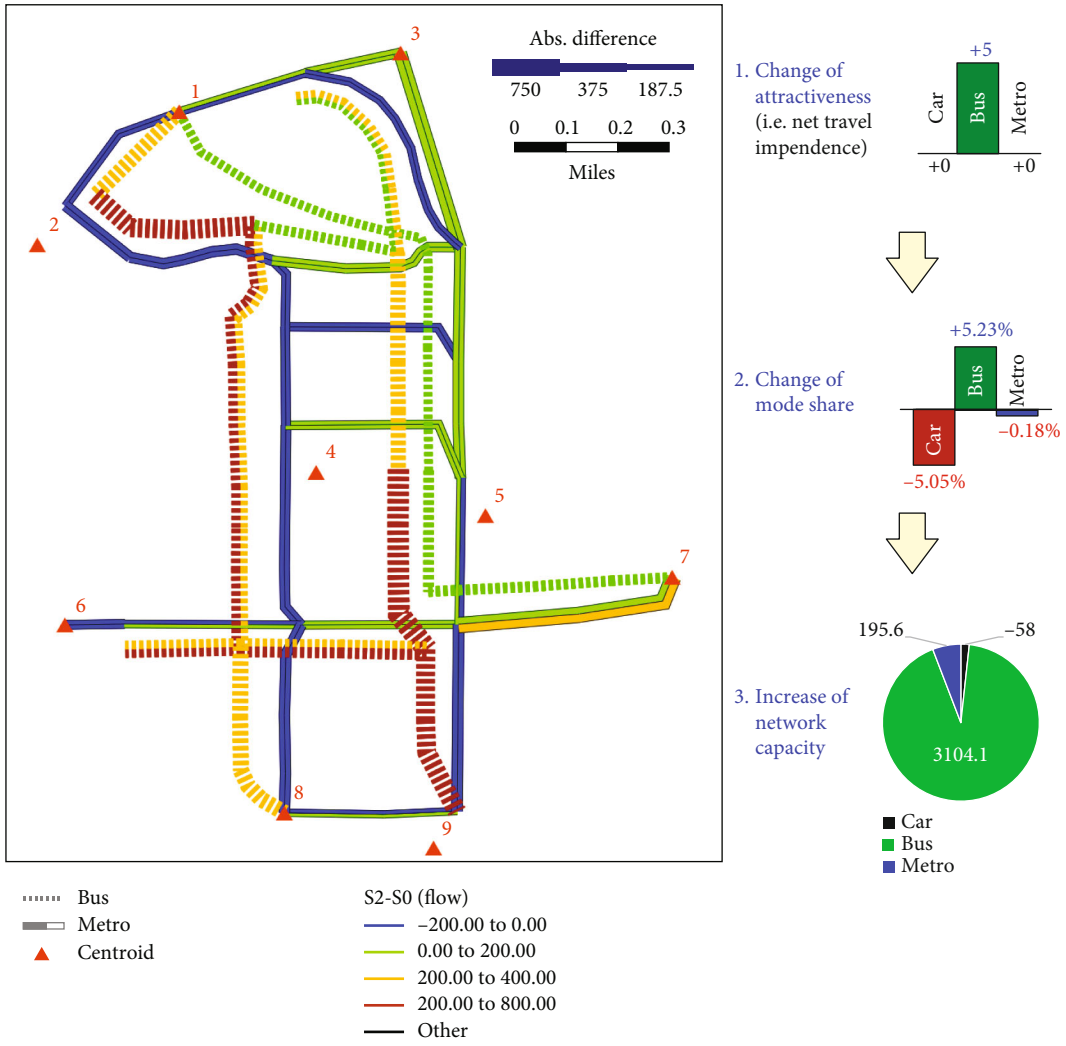

Figure 16: Comparison of maximum flow patterns before and after increasing bus attractiveness.

the metro line No.3 is a new built line. The effectiveness of constructing metro line No. 3 will be embodied according to the network capacity evaluation results. With the new metro line, the evaluation results show that the reserve network capacity is improved from $\mu = 1.48$ to 1.62, which means adding a new metro line can greatly increase the multimodal network capacity. Besides, the metro share rate increases from 8.91% to 17.41%. Figure 17 shows the changes in the multimodal OD distributions after the construction of metro line No. 3. The OD pairs connecting centroid 1, 4, 8, and 9 have a great change on demand patterns since these OD pairs are benefited from the new metro line. It also shows that the growth of the total network capacity is mostly contributed by the new metro line, which bears 4,474 trips/h travel demand at the maximum demand situation. On the contrary, the same OD pairs (in red zones) for car and bus modes show a decline in demand.

Moreover, Figure 18 depicts the changes in OD demand by each mode. Overall, due to the new metro line, the total demands of car and metro, respectively, increase by 912 trips/h and 4,887 trips/h, while the total bus demand decreases by 1,241 trips/h. By decomposing the changes into individual OD pairs, we note that the metro demand growth almost occurs at the OD pairs connected by the new metro line. For these OD pairs, the demands of car and bus are attracted to the metro and show significant reductions. Also, we find that more percentage of bus demand shifts to the metro in comparison to car demand (see Figure 18). This is interpreted by the nested structure of the NL model for mode choice. With the new metro line, the total share rate of bus and metro is increased (as Table 4). However, the bus users are easier to shift to metro than the car drivers, because both bus and metro are public transport and are considered in the same nest (effect of mode similarity). Thereby, the bus mode shows a total net loss (-1,241 trips/h) caused by the new metro line. In addition, as the metro system is more competitive in medium to long-distance, Figure 18 shows that long trips on the road network (by car and bus) are reduced obviously after building the new line. Consequently, the road network will have more residual space and

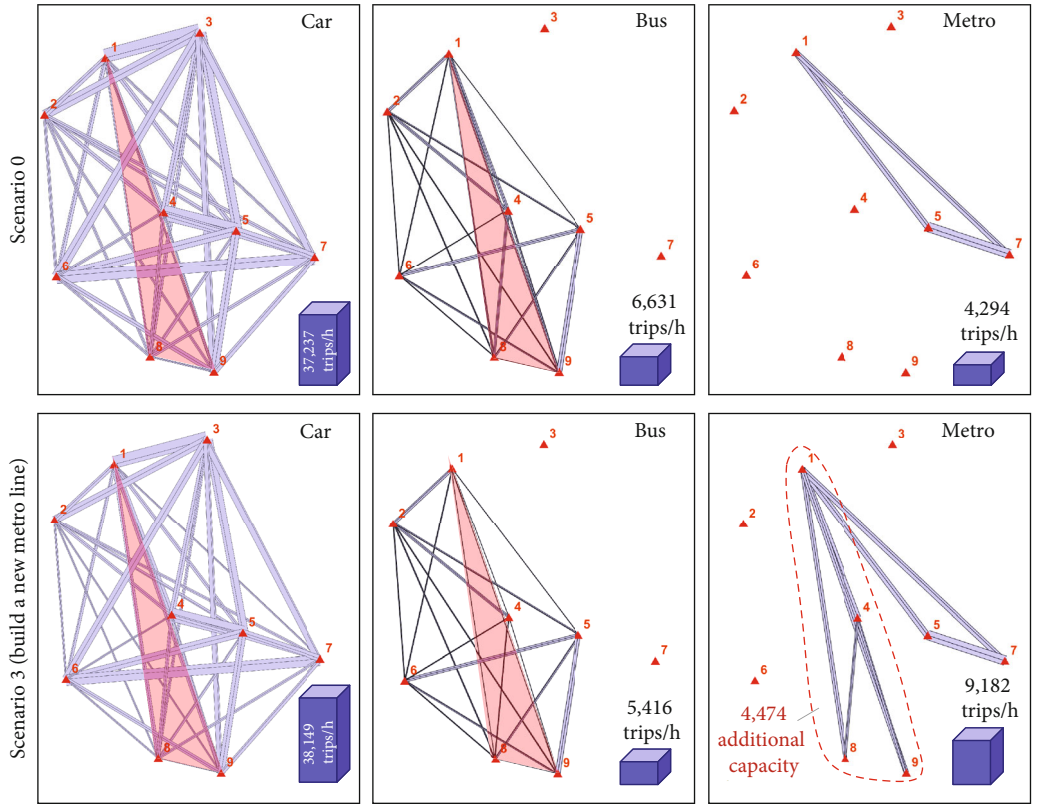

Figure 17: Maximum demand by multimodal OD before and after building new metro line.

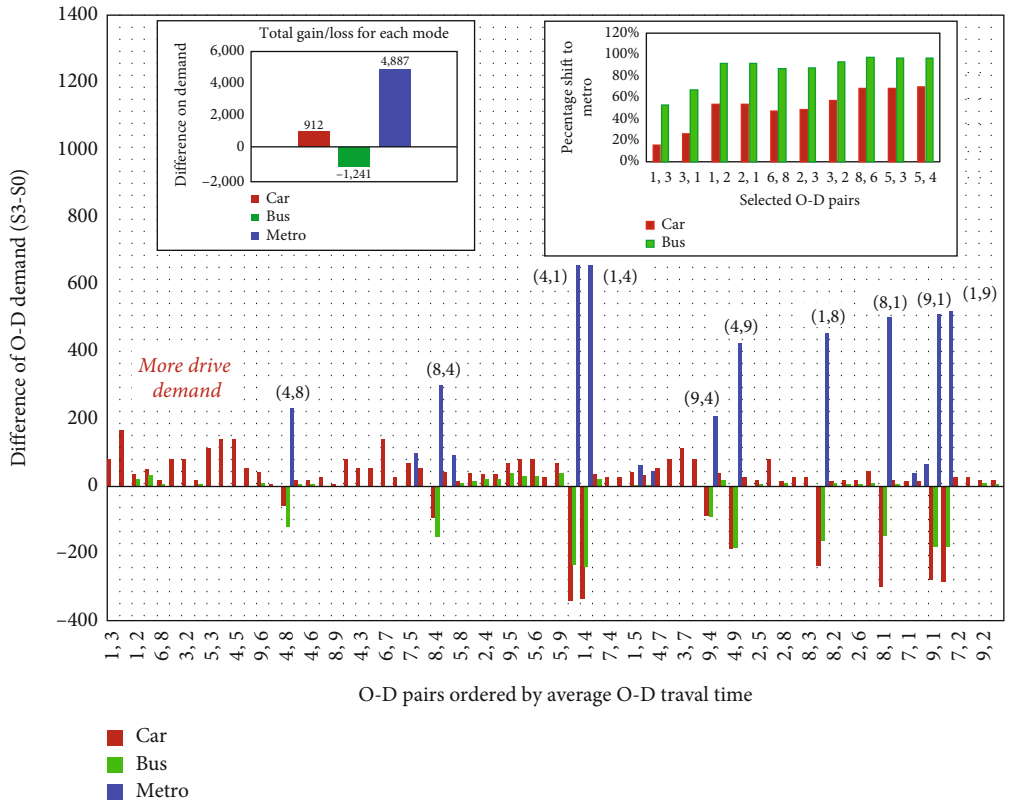

Figure 18: Comparison of multimodal OD demands before and after building new metro line.

Table 4: Network capacity evaluations under different scenarios.

Scenario	Total network capacity (multiplier)	Mode share rates (car/bus/metro)
0	1.48	77.32%/13.77%/8.91%
1	1.27 (↓)	77.84%/13.39%/8.77%
2	1.58 (↑)	72.27%/19.00%/8.73%
3	1.62 (↑)	72.32%/10.27%/ 17.41%

hence can take over more drive demand in short trips. Hence, the total car demand increases slightly from the overall result.

In summary, the network capacity assessment under the four scenarios are reported in Table 4. From Scenario 1, adding a new road may reduce the capacity of the multimodal transportation network. Enhancing network capacity and increasing alternative diversity may not be always consistent. In addition, utilizing public transport to share more travel demand is a recommended choice to expand the network spare capacity. This can be realized by either encouraging public transport (Scenario 2) or improving the transit network (Scenario 3).

5. Conclusions

This study focused on the modelling of mode choice and route choice in the lower-level of the bilevel multimodal network capacity model, and extended the network capacity analysis to consider multiple travel modes. Thus, a CMSTA model is formulated step by step originating from the stochastic user equilibrium with elastic demand. In the CMSTA, the route overlapping problem is captured by using the PSL model, and the mode similarity is characterized by the NL model. Besides, an alternative formulation of the MP-formulated network capacity models was derived in this study, by which the objective function is associated with the entropy maximization theorem and dual variables of the constraints are associated with the EPCs of the travel modes. By extending the reserve capacity concept, the multimodal network capacity model can be easily solved with the given SAB algorithm. At last, numerical results showed that the proposed multimodal network capacity model can capture both mode similarity and route overlapping lying in the multimodal transportation system, and thus further improve the network capacity results; it can evaluate how planning or management strategies (e.g., adding new links or mode options, improve modal attractive) change the mode share rates and further benefit for network-wide capacity.

It has been noticed that, adding new links may lead to the capacity paradox, which causes the reduction of the network-wide capacity even though the travel alternative diversity is increased; adding new modes generally can improve the network capacity although the capacity paradox may occur in some extreme condition; considering route overlap or mode similarity will increase the EPC for the group of the correlated route or mode alternatives, which changes the mode share rates and further impacts the network capacity evaluation. In addition, from the real case study, both encouraging public transport (i.e., increase the attractiveness of buses) and constructing a new metro line (if budget is enough) can be an effective way to enhance multimodal transportation network capacity.

Data Availability

The data used to support the findings of this study are included within the article.

Conflicts of Interest

The authors declare that they have no conflicts of interest.

Acknowledgments

The work was jointly supported by research grants from Jiangsu University Philosophy and Social Science Research Project (2019SJA0471), the Natural Science Foundation of China (52002113), Jiangsu Natural Science Foundation (BK20200526), and the Fundamental Research Funds for the Central Universities (B220202009).

References

[1] S. Wang, Z. Pu, Q. Li, and Y. Wang, "Estimating crowd density with edge intelligence based on lightweight convolutional neural networks," *Expert Systems with Applications*, vol. 206, p. 117823, 2022.

[2] Y. Zhuang, Z. Pu, H. F. Yang, and Y. Wang, "Edge-artificial intelligence-powered parking surveillance with quantized neural networks," *IEEE Intelligent Transportation Systems Magazine*, vol. 2, p. 16, 2022.

[3] W. Li, Z. Pu, Y. Li, and X. Ban, "Characterization of ridesplitting based on observed data: a case study of Chengdu, China," *Transportation Research Part C: Emerging Technologies*, vol. 100, pp. 330–353, 2019.

[4] Y. Zhuang, Z. Pu, J. Hu, and Y. Wang, "Illumination and temperature-aware multispectral networks for edge-computing-enabled pedestrian detection," *IEEE Transactions on Network Science and Engineering*, vol. 9, no. 3, pp. 1282–1295, 2021.

[5] X. Xu, A. Chen, S. Jansuwan, C. Yang, and S. Ryu, "Transportation network redundancy: complementary measures and computational methods," *Transportation Research Part B: Methodological*, vol. 114, pp. 68–85, 2018.

[6] H. Yang and M. G. H. Bell, "A capacity paradox in network design and how to avoid it," *Transportation Research Part A: Policy and Applications*, vol. 32, no. 7, pp. 539–545, 1998.

[7] X. Jiang, M. Du, and H. Liu, "Assessing urban road network capacity considering parking supply and parking pricing," *Journal of Advanced Transportation*, vol. 2020, Article ID 8820680, 17 pages, 2020.

[8] J. Zhou, M. Du, and A. Chen, "Multimodal urban transportation network capacity model considering intermodal transportation," *Transportation Research Record*, 2022.

[9] H. Yang, M. G. H. Bell, and Q. Meng, "Modeling the capacity and level of service of urban transportation networks," *Transportation Research Part B-Methodological*, vol. 34, no. 4, pp. 255–275, 2000.

[10] Y. Asakura, "Maximum capacity of road network constrained by user equilibrium conditions," in *Paper presented at the 24th Annual Conference of the UTSG*, 1992.

[11] S. C. Wong and H. Yang, "Reserve capacity of a signal-controlled road network," *Transportation Research Part B: Methodological*, vol. 31, no. 5, pp. 397–402, 1997.

[12] Z. Y. Gao and Y. F. Song, "A reserve capacity model of optimal signal control with user-equilibrium route choice," *Transportation Research Part B-Methodological*, vol. 36, no. 4, pp. 313–323, 2002.

[13] P. Kasikitwiwat and A. Chen, "Analysis of transportation network capacity related to different system capacity concepts," *Journal of the Eastern Asia Society of Transportation Studies*, vol. 6, pp. 1439–1454, 2005.

[14] J. Wang, M. Du, L. Lu, and X. He, "Maximizing network throughput under stochastic user equilibrium with elastic demand," *Networks and Spatial Economics*, vol. 18, no. 1, pp. 115–143, 2018.

[15] H. Ceylan and M. G. H. Bell, "Reserve capacity for a road network under optimized fixed time traffic signal control," *Journal of Intelligent Transportation Systems*, vol. 8, no. 2, pp. 87–99, 2004.

[16] A. Chen, H. Yang, H. K. Lo, and W. H. Tang, "Capacity reliability of a road network: an assessment methodology and numerical results," *Transportation Research Part B-Methodological*, vol. 36, no. 3, pp. 225–252, 2002.

[17] S.-W. Chiou, "Reserve capacity of signal-controlled road network," *Applied Mathematics and Computation*, vol. 190, no. 2, pp. 1602–1611, 2007.

[18] L. Cheng, M. Du, X. Jiang, and H. Rakha, "Modeling and estimating the capacity of urban transportation network with rapid transit," *Transport*, vol. 29, no. 2, pp. 165–174, 2014.

[19] Y. Zheng, X. Zhang, and Z. Liang, "Multimodal subsidy design for network capacity flexibility optimization," *Transportation Research Part A: Policy and Practice*, vol. 140, pp. 16–35, 2020.

[20] Z. Liu, Z. Wang, Q. Cheng, R. Yin, and M. Wang, "Estimation of urban network capacity with second-best constraints for multimodal transport systems," *Transportation Research Part B: Methodological*, vol. 152, pp. 276–294, 2021.

[21] J. Ye, Y. Jiang, J. Chen, Z. Liu, and R. Guo, "Joint optimisation of transfer location and capacity for a capacitated multimodal transport network with elastic demand: a bi-level programming model and paradoxes," *Transportation Research Part E: Logistics and Transportation Review*, vol. 156, p. 102540, 2021.

[22] P. Zhang, H. Yue, C. Shao, X. Zhang, and B. Ran, "Modelling the road network capacity considering residual queues and connected automated vehicles," *IET Intelligent Transport Systems*, vol. 16, pp. 1–8, 2021.

[23] D. Watling, "Asymmetric problems and stochastic process models of traffic assignment," *Transportation Research Part B: Methodological*, vol. 30, no. 5, pp. 339–357, 1996.

[24] M. Florian and S. Nguyen, "A combined trip distribution modal split and trip assignment model," *Transportation Research*, vol. 12, no. 4, pp. 241–246, 1978.

[25] M. Abdulaal and L. J. LeBlanc, "Methods for combining modal split and equilibrium assignment models," *Transportation Science*, vol. 13, no. 4, pp. 292–314, 1979.

[26] E. Fernandez, J. De Cea, M. Florian, and E. Cabrera, "Network equilibrium models with combined modes," *Transportation Science*, vol. 28, no. 3, pp. 182–192, 1994.

[27] R. Garcia and A. Marin, "Network equilibrium with combined modes: models and solution algorithms," *Transportation Research Part B: Methodological*, vol. 39, no. 3, pp. 223–254, 2005.

[28] N. Oppenheim, *Urban Travel Demand Modeling*, John Wiley and Sons Inc, New York, 1995.

[29] Z. X. Wu and W. H. K. Lam, "Combined modal split and stochastic assignment model for congested networks with motorized and nonmotorized transport modes," *Transportation Research Record*, vol. 1831, no. 1, pp. 57–64, 2003.

[30] O. A. Nielsen, A. Daly, and R. D. Frederiksen, "A stochastic route choice model for car travellers in the Copenhagen region," *Networks and Spatial Economics*, vol. 2, no. 4, pp. 327–346, 2002.

[31] Y. Sheffi, *Urban Transportation Networks: Equilibrium Analysis with Mathematical Programming Methods*, Prentice-Hall, Englewood Cliffs, NJ, 1985.

[32] M. Ben-Akiva and M. Bierlaire, "Discrete choice methods and their applications to short term travel decisions," in *Handbook of Transportation Science*, R. W. Halled, Ed., Kluwer Publishers, 1999.

[33] Z. Pu, Z. Cui, J. Tang, S. Wang, and Y. Wang, "Multi-modal traffic speed monitoring: a real-time system based on passive Wi-Fi and bluetooth sensing technology," *IEEE Internet of Things Journal*, vol. 9, no. 14, pp. 12413–12424, 2021.

[34] X. Xu and A. Chen, "C-logit stochastic user equilibrium model with elastic demand," *Transportation Planning and Technology*, vol. 36, no. 5, pp. 463–478, 2013.

[35] H. Yang, "Sensitivity analysis for the elastic-demand network equilibrium problem with applications," *Transportation Research Part B: Methodological*, vol. 31, no. 1, pp. 55–70, 1997.

[36] C. Sun, L. Cheng, S. Zhu, and Z. Chu, "Multiclass stochastic user equilibrium model with elastic demand," *Transportation Research Record*, vol. 2497, no. 1, pp. 1–11, 2015.

[37] M. J. Maher, "Stochastic user equilibrium assignment with elastic demand," *Traffic Engineering & Control*, vol. 42, no. 5, pp. 163–167, 2001.

[38] A. Papola, "Some developments on the cross-nested logit model," *Transportation Research Part B-Methodological*, vol. 38, no. 9, pp. 833–851, 2004.

[39] T. Akamatsu and O. Miyawaki, "Maximum network capacity problem under the transportation equilibrium assignment," *Infrastructure Planning Review*, vol. 12, pp. 719–729, 1995.

[40] A. Chen and P. Kasikitwiwat, "Modeling capacity flexibility of transportation networks," *Transportation Research Part A-Policy and Practice*, vol. 45, no. 2, pp. 105–117, 2011.

[41] M. Du, X. Jiang, and L. Cheng, "Alternative network robustness measure using system-wide transportation capacity for identifying critical links in road networks," *Advances in Mechanical Engineering*, vol. 9, no. 4, 2017.

[42] H. Bar-Gera, F. Hellman, and M. Patriksson, "Computational precision of traffic equilibria sensitivities in automatic network design and road pricing," *Procedia - Social and Behavioral Sciences*, vol. 80, pp. 41–60, 2013.

[43] H. X. Liu, X. He, and B. He, "Method of successive weighted averages (mswa) and self-regulated averaging schemes for solving stochastic user equilibrium problem," *Networks and Spatial Economics*, vol. 9, no. 4, pp. 485–503, 2007.

[44] M. Du and A. Chen, "Sensitivity analysis for transit equilibrium assignment and applications to uncertainty analysis," *Transportation Research Part B: Methodological*, vol. 157, pp. 175–202, 2022.

[45] A. V. Fiacco, *Introduction to Sensitivity and Stability Analysis in Nonlinear Programming*, Acedemic Press, New York, 1983.

[46] T. L. Friesz, R. L. Tobin, H. J. Cho, and N. J. Mehta, "Sensitivity analysis based heuristic algorithms for mathematical programs with variational inequality constraints," *Mathematical Programming*, vol. 48, no. 1-3, pp. 265–284, 1990.